SÜMEYYE BAHÇECİ

M.S. Thesis in Chemistry

July- 2010

POLYRADICAL BASED ORGANIC ELECTRODES TO BE USED IN ORGANIC PLASTIC BATTERIES

by

Sümeyye BAHÇECİ

July 2010

POLYRADICAL BASED ORGANIC ELECTRODES TO BE USED IN ORGANIC PLASTIC BATTERIES

by

Sümeyye Bahçeci

A thesis submitted to

the Graduate Institute of Sciences and Engineering

of

Fatih University

in partial fulfillment of the requirements for the degree of

Master of Science

in

Chemistry

July 2010
Istanbul, Turkey

APPROVAL PAGE

I certify that this thesis satisfies all the requirements as a thesis for the degree of Master of Science.

_____

Prof. Dr. Ayhan BOZKURT
Head of Department

This is to certify that I have read this thesis and that in my opinion it is fully adequate, in scope and quality, as a thesis for the degree of Master of Science.

_____

Assist. Prof. Dr. Burak ESAT
Supervisor

Examining Committee Members

Prof. Dr. Naz Mohammed AGH-ATABAY _____

Assoc. Prof. Dr. Bayram ÜNAL _____

Assist. Prof. Dr. Burak ESAT _____

It is approved that this thesis has been written in compliance with the formatting rules laid down by the Graduate Institute of Sciences and Engineering.

_____

Assoc. Prof. Dr. Nurullah ARSLAN
Director

July 2010

POLYRADICAL BASED ORGANIC ELECTRODES TO BE USED IN ORGANIC PLASTIC BATTERIES

Sümeyye BAHÇECİ

M.S. Thesis – Chemistry
July 2010

Supervisor: Assist. Prof. Dr. Burak ESAT

ABSTRACT

Organic Radical Batteries (ORBs) are good candidates for the rechargeable battery technology to provide high energy densities along with a good performance during a large number of charge-discharge cycles and being non-toxic. Organic radical containing polymers (redox-active polymers) are used as electrode active materials for these kind of batteries.

In this study, alkyl substituted acetylenic monomers including TEMPO stable radicals were synthesized. Fischer esterification and nucleophilic substitution reactions were applied to obtain related monomers. Then their polymers, TEMPO bearing poly(alkyl substituted acetylenes) were synthesized by using $[Rh(nbd)Cl]_2$ catalyst with two different cocatalysts (Et_3A and LDA). Synthesized monomers were characterized via FT-IR, ^{1}H-NMR and UV spectroscopy, mass spectrometry, elemental analysis, and ESR. The polymers obtained were analyzed by FT-IR, ESR and UV spectroscopy, GPC, DSC, TGA, CV. Finally, coin-sized cells were constructed by using these polymers as cathodes and tested for their charging and discharging properties.

Keywords: Organic, polymer, radical, secondary battery, electrode-active material

ORGANİK PLASTİK PİLLERDE KULLANILACAK POLİRADİKAL BAZLI ORGANİK ELEKTRODLAR

Sümeyye BAHÇECİ

Yüksek Lisans Tezi – Kimya
Haziran 2010

Tez Yöneticisi: Yrd. Doç. Dr. Burak ESAT

ÖZ

Organik Radikal Piller (ORB) çok sayıda şarj-deşarja döngüsü boyunca iyi bir performansla sağladıkları yüksek enerji yoğunluklarıyla ve zehirsiz oluşlarıyla şarj edilebilir pil teknolojisi için iyi birer adaydırlar. Bu tür pillerde organik radikal içeren polimerler (redoks-aktif polimerler) elektrot aktif materyal olarak kullanılmaktadır.

Bu çalışmada, TEMPO kararlı radikalini taşıyan alkil asetilen içerikli monomerler sentezlenmiştir. Fischer esterleşme reaksiyonu ve nükleofilik yer değiştirme tepkimeleri kullanılmıştır. Bu monomerlerden, farklı kokataliz eşliğinde (LDA ve Et_3A) $[Rh(nbd)Cl]_2$ katalizörü kullanılarak TEMPO radikali taşıyan alkil içerikli poliasetilenler sentezlenmiştir. Elde edilen monomerler FT-IR, ^{1}H-NMR, UV spektroskopisi, kütle spektrometrisi, elementel analiz ve ESR kullanılarak karakterize edilmiştir. Polimerlerin karakterizasyonunda ise FT-IR, ESR ve UV spektroskopisi, GPC, DSC, TGA ve CV kullanılmıştır. Son olarak, bu polimerler katodda kullanılarak düğme piller yapılıp ve şarj ve deşarj özellikleri incelenmiştir.

Anahtar Kelimeler: Organik, polimer, radikal, ikincil pil, elektrod-aktif malzeme

dedicated to my wonderful parents…

ACKNOWLEDGEMENT

I express sincere appreciation to Assist. Prof. Dr. Burak Esat for his guidance, helpful and stimulating suggestions and insight throughout the research and efforts for writing this thesis.

I also want to thank my lab mate Muhammet Aydın for his assistance of the GPC, ESR and mass analysis measurements in GYTE (Gebze Institute of Technology).

I am very gratefull to Prof. Dr. Ayhan Bozkurt and Res. Asst. Mehmet Şenel to open the door of their laboratories and let me to use their important lab instruments. And I also want to express my thanks to Assoc. Prof. Dr. Abdülhadi Baykal, Res. Asst Sevim Ünügür Çelik and Hamide Aydın for XRD, conductivity, TGA and DSC measurements.

In particular I would like to acknowledge the help of Prof. Dr. Naz Mohammed AGH ATABAY and Assist. Prof. Dr. Ramazan Öztürk for their support, general advice and positive thoughts.

I would also like to thank Ayşe Demir for her helpful thoughts, interesting ideas, sharing her experiences. She has a fantastic nature, I believe that she will be a good scientist in the future.

And thanks to all other colleagues Bahar Birsöz, Şeyda Karaman and Hilal Doğan for their moral support during my research.

And my dear colleageous, Serhat Gündüz and Deniz Sinirlioğlu, they are good men. I thank them for their pleasant nature, kindly behavior, and for technical supports.

I want to express my special thanks to Murat Sertkol who always strengthened my morale by standing with me in all situations. I am very gratefull to him for his contributions to my research by working me at weekends, for his technical support during writing this thesis and discussing me some important subjects.

My sincere thanks also goes to TUBITAK (The Scientific and Technological Research Council of Turkey) & Fatih University for funding my thesis.

Finally, I would like to express a deep sense of gratitude to my parents, especially to my dearest Mom, who has always thought me in her bad days during her cancer treatment and for her constant love, encouragement, and moral support.

TABLE OF CONTENTS

LIST OF SCHEMES

LIST OF FIGURES

LIST OF TABLES

LIST OF SYMBOLS AND ABBREVIATIONS

ORB	:	Organic Radical Battery
NMR	:	Nuclear Magnetic Resonance
FTIR	:	Fourier Transform Infrared Spectroscopy
GPC	:	Gel Permission Chromatography
DSC	:	Differantial Scanning Calorimetry
ESR	:	Electron Spin Resonance
CV	:	Cyclic Voltammetry
TGA	:	Thermal Gravimetric Analysis
Tg	:	Glass Transition Temperature
TLC	:	Thin Layer Chromatography
TEMPO	:	4-hydroxy-TEMPO
PTMA	:	Poly(2,2,6,6-tetramethylpiperidinyloxy methacrylate)
Et_3N	:	Triethylamine
NaH	:	Sodium hydride
CH_2C_2	:	Dichlorometan
THF	:	Tetrahydrofuran
DMF	:	Dimethylformamide
LDA	:	Lithium diisopropylamide
DEC	:	Diethyl carbonate
EC	:	Ethylene carbonate
EDCl·HCl	:	Ethyl-3-(3-dimethyllaminopropyl)carbodiimide hydrochloride
DMAP	:	4-Dimethylaminopyridine
NMP	:	N-methyl-2-pyrrolidone
AIBN	:	Azobisisobutyronitrile
ITO	:	Indium Tin Oxide
$[Rh(NBD)Cl]_2$	:	Rhodium norbornadiene chloride dimer
TBAP	:	Tetramethyl ammonium perclorate
PVDF	:	Polyvinylidene Fluorid

CHAPTER 1

INTRODUCTION

The growing interest in using redox-active polymers (including organic radical containing polymers) as electroactive elements for energy storage and charge transport in rechargeable batteries has led to the displacement of inorganic battery materials with more cheaper, non-toxic and benign organic ones that are able to provide high energy densities along with a good performance during a large number of charge-discharge cycles.

Organic Radical Battery (ORB) is a new type of rechargeable battery that utilizes the reversible redox active radical polymers as at least one of its electrodes. They are characterized by their fast kinetics of electrode reactions. Generally, the oxygen centered, commercially available stable nitroxide radicals, such as 2,2,6,6-tetramethylpiperidine-1-oxyl (TEMPO) are chosen for this kind of applications. Organic polymers containing these radical moities lead to a new electrode-active materials for application in rechargeable batteries. Because electrochemical studies of the nitroxide containing polymers have showed that the nitroxide center displays reversible redox behavior attributable to oxidation of the nitroxide radical and reduction of the corresponding oxoammonium form.

The first attempt on the use of an organic radical as an electrode-active or charge storage material in lithium battery was performed by Nakahara et al. in 2002 [1]. PTMA (poly(2,2,6,6-tetramethylpiperidinyloxy-4-yl methacrylate), was the first generation organic compound as a cathode active material in lithium battery polymer. Since then, a few more studies were published by Nishide et al [2-5]. Organic polymers which have

TEMPO radical bound to the aliphatic or nonconjugated backbone show excellent properties such as rapid electron transfer, high density of charges stored, transparent film formability and ability of controlling the redox potential based on the substituent effect in organic molecules. The most striking feature is the efficient electron hopping within the polymer film allows fast electron injection and rejection on the electrode.

Since PTMA is an insulator, the cathode composition generally consists of only a small proportion of active material, the major portion being the conductive agent like carbon and its derivatives. More recently, Nishide and coworkers introduced TEMPO radical into a conductive polymer, substitued polyacetylenes and it leaded to new functional materials based on reversible effect of stable organic radicals and main chain of conjugated polyacetylene units. Substitutued polyacetylenes exhibit unique properties such as semiconductivity, paramagnetism, helix formation, electrochromism, high gas permeability-$O_{2(g)}$. A number of conducting polymers [6,7] were synthesized and have been recently studied as material for not only rechargeable batteries but also photovoltaic devices [8-11], and electrochromic (EC) cell [12-14]. Especially, the electrochemical properties of conducting polymers as organic semiconductors for light emitting diodes (OLEDS) and organic thin film solar cells have been intensively studied.

Energy density is one of the most significant points for rechargeable batteries. There is a variety of inorganic based secondary batteries which have been developed and commercialized to provide consumer demands: lead-acid (Pb-acid) and Nickel-Cadmium (Ni-Cd) batteries are the most known ones. For increasing the specific energy (which gives a measure of the energy output per unit mass in Wh/kg or Wh/L), researchers then focused on the safe storage of the smallest energy carrying ions, the hydrogen and lithium. Nickel-Metal Hydride (Ni-MH) and Lithium-ion (Li-ion) have been developed based on this concept. Figure 1.1 shows the superior characteristics of Li-ion batteries over the others.

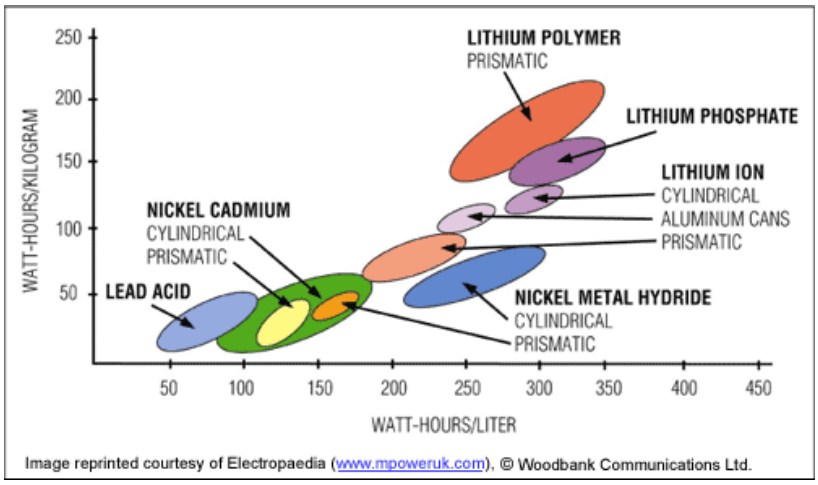

Figure 1.1. Energy characteristics of four common secondary batteries [15].

There exist two types of lithium batteries, classified based on the anode material: (a) lithium metal type where the anode is pure lithium metal or its alloy, and (b) Li-ion type where different lithium intercalation compounds like graphite are used as anodes. The idea of a rechargeable lithium cell based on Li^+ insertion reactions has been studied since the early 1970s, and numerous lithium insertion electrodes have been introduced to date. The reason for their widespread application is related with their simple and reversible electrochemical insertion reactions. This term refers to a host/guest solid-state redox reaction involving electrochemical charge transfer between the electrolyte and solid host. The mobile guest ions, Li^+ delivered from Li containing electrolyte, generally $LiClO_4$ or $LiPF_6$ transport into the structure of the solid host, which is mixed electronic and ionic conductor. Generally, these insertion reactions are highly reversible. However, the relatively slow transport of guests in the solid host limits the rate capability of the charge/discharge reaction. For example, the cell reactions of rechargeable aqueous batteries such as metal hydride/NiOOH or Zn/MnO_2 involve the reversible electroinsertion of H^+ into metal hydrid [16-19] except for protons no cations other than the small Li^+ can diffuse so easily into solids by insertion reactions. The application of this technology was developed commercially by Sony in 1991, with both the anode and cathode materials operating as “host lattices” for lithium ions.

Thus, $LiCoO_2$ with a layered structure is the most widely used cathode material with its excellent electrochemical cycling stability. It displays a satisfactory performance with the largest energy density, a practical discharge capacity of ~145 mAh/g and long cycle lives (>1000 cycles).

The main problems related with this electrode material is its high cost, toxicity, the large volume change that occurs during redox process which limits the attainment of full reversibility. Another problem is also the slowness of reversible cycling of $LiCoO_2$, as a result leads to limitations in the high-rate capability of the batteries.

Recently, new approaches for the development of new cathode materials have been dealt by the researchers. The materials that are cheap, non-toxic, and most importantly that can provide a high-rate capability leading to fast acceleration and efficient regeneration in high-power applications are demands of the future.

Test batteries have been demonstrated and it has been proved that plastic batteries using organic electrodes have intrinsic advantages over lithium –ion batteries, because of the flexibility of organic materials and having a large variability to increase the potential properties by taking advantage of substituent effect on the polymer backbone.

In the light of above discussions, organic radical batteries (ORBs) are emerging as promising, environmentally benign and high rate capable power sources to satisfy human needs. Under this context, this thesis focused on the synthesis of new organic polymers with pendant electroactive stable organic radicals and preparation of the new rechargeable coin-size batteries based on these polymers as the cathode.

CHAPTER 2

ORGANIC RADICAL POLYMERS AND π-CONJUGATED POLYMERS

Radical polymers are aliphatic or conjugated polymers bearing organic stable radicals as pendant groups per repeating unit. They are emerging a new class of electroactive materials useful for consumer demands. They have been studied for a long time by many researchers and reported in many papers. In this section, fundamental of the organic radical polymers and conjugated polymers will be described.

2.1. ORGANIC RADICAL MOLECULES AND POLYMERS

Organic radical molecules are redox active attributable to the oxidation and reduction to corresponding molecules and this character makes them available for active material for rechargeable batteries. Generally, organic radicals often appear as intermediates in photochemical and thermal reactions and are also known to initiate and propagate polymerization and combustion reactions. The short-lived and highly reactive radicals can be converted to stable molecules through dimerization or redox reactions with other molecules, solvents, or molecular oxygen. For example, the methyl radical easily forms ethane ($2CH_3\bullet \rightarrow CH_3\text{-}CH_3$) by dimerization. Thus the organic molecular radicals had been hitherto classified as unstable and intractable materials. Since their stability and redox abilities are generally influenced by the degree of delocalization and the substituent effects, stable organic radicals in ambient atmosphere can be designed and synthesized.

Chemical stabilization can be increased by modifying the structure enough to be separated from the reaction mixture. It can be achieved by making it physically difficult to react with other molecules via sterically protected structures around the radical centers or the unpaired electrons and/or by resonance structures involving the unpaired electrons. For example, t-butyl unit is a good protecting group for phenoxy or nitroxy units. Based on this theory, hundreds of stable organic radicals are known and commercially sold. Some of them are stable even in the open atmosphere such as 2,2,6,6-tetramethylpiperidinyl-N-oxy (TEMPO) radical. Some of these persistent radicals are shown in Figure 2.1. Nitrogen centered diphenylpicrylhydrazyl (DPPH) and triphenylaminium cationic radicals, oxygen-centered 2,4,6-tri-t-butylphenoxyl, galvinoxyl, nitrogen-oxygen centered nitronyl nitroxide, and 2,2,6,6-tetramethyl-1-piperidinyloxy (TEMPO) radicals and carbon centered tris(pentachlorophenyl)methyl and bis(diphenylenepropenyl)phenylmethyl radicals are some of them [20,21].

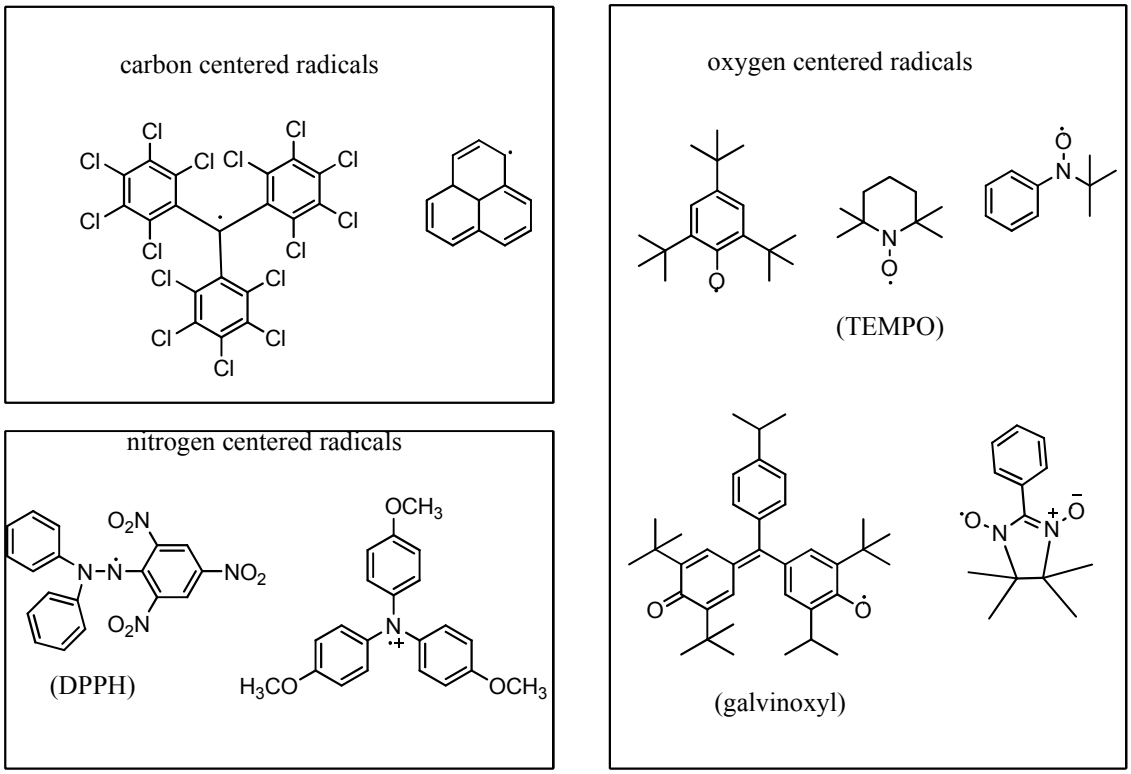

Figure 2.1. Chemical structures of stable radical molecules.

Stable radicals have been used as the spin labels for biomolecules or as the radical scavengers of organic materials and biological systems. Moreover, organic radical molecules provide an advantage as a side chain on organic polymers and

frequently employed as functional materials such as polymeric stabilizers [21,22], oxidants of alcohols [23-26] and spin and charge storage materials [27-30]. Among them nitroxyl radicals such as TEMPO and PROXYL are well known and have found many applications in these fields. Because they exhibit fast and reversible electrochemical redox reaction. Thus, organic radical polymers have great potential for using their intrinsic properties.

The radical polymers which show reversible redox reactions were studied extensively in the 1970s as redox reagents or redox resins, which catalyze the oxidative and/or reductive reactions of organic compounds [31-35]. For example, poly(acrylic acid)-combined TEMPOs were synthesized and studied as a catalytic reagent for the oxidation of alcohols into aldehydes and ketones [36]. Electrochemical studies of these polymers have revealed that the nitroxide center displays reversible redox behavior attributable to oxidation of the nitroxide radical and reduction of the corresponding (TEMPO) oxoammonium form, which is the molecular basis for the use in redox reagents.

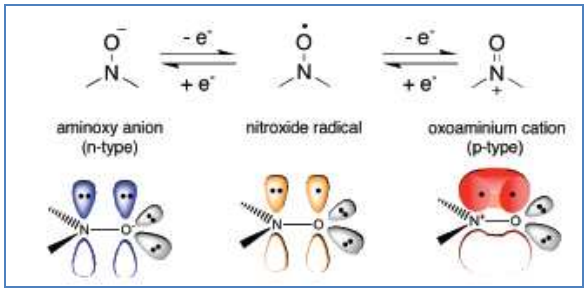

Figure 2.2. Electrochemical redox process of nitroxide radicals [5].

2.1.1. REDOX POLYMERS (POLYMERS BEARING REDOX CENTERS)

Redox polymers is a term used for a group of polymers with nonconjugated backbone and having localized redox centers in pendant groups. The redox centers, not the polymer chain, govern the redox behavior. Conductivity arises when these centers can exchange charge, e.g., on account of mixed valency [37-39]. In contrast, the polymers that have a conjugated backbone where optional groups (substituents) merely modify the spectrum of redox states offered by the polymer chain**.**

Ferrocene (Fc) [2,40,41], carbazole groups (Cz) [42], tetrathiafulvalene (TTF) [43], triphenylamine (TPA) [44,45], polyoxyphenazine, and the adduct-forming polyamides

and polyvinyl polymers are the general types of redox polymers. The structures of this redox polymers are showed in Fig. 2.3.

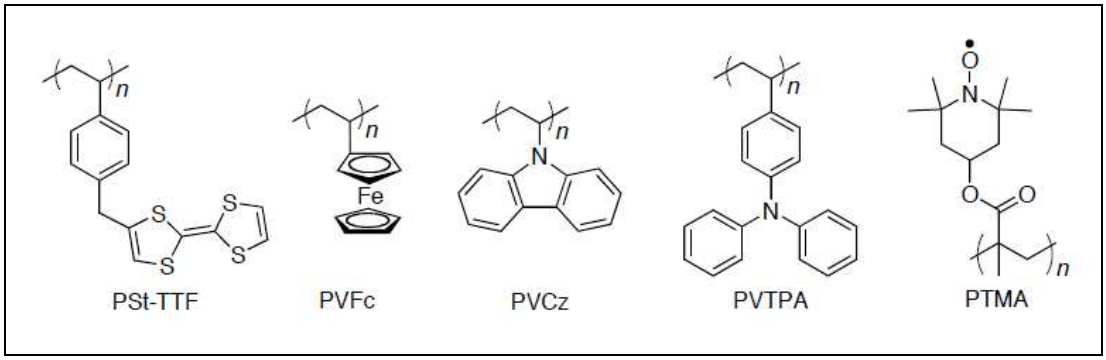

Figure 2.3. A series of redox polymers.

Tetrathiafulvalene (TTF)-functionalized polystyrene film was used by Kaufman *et al.* for the preparation of electroactive modified electrode. It showed the same redox changes in TTF in THF solution. Facile electronic conduction through the amorphous film was reported, ascribed to the electron exchange between the closely spaced TTF groups. Counter-ion movement ($TTF^{+}ClO_4^{-}$) through the polymer matrix accompanies the electron movement along these groups. Cycling behavior under CV conditions was found to be excellent.

Poly(vinylferrocene) (PVFc) dissolved in dichloromethane was transformed to the insoluble doped polymer (polyethylene with ferricenium salt and ferrocene as mixed-valence substituents) through potentiostatic oxidation by Shirota *et al* [38]. This process led to precipitation of polymer on the electrode. Iwakura *et al* [46] cast their films from CH_2Cl_2 solutions and tested by CV, but also measured charge-discharge curves in half cells. And the obtained data showed that they exhibit high power capability, in contrast to the conducting polymer.

Like (PVFc), poly(N-vinylcarbazole) (PVCz) was generally described due to its preparation. It was prepared electrochemically and combined with Li in cells. Since its redox reaction was coupled the side reaction such as dimerization, it exhibits poor power capability.

It was realized that in the late of 1980s, disulphide compounds, so common in proteins involving cysteine-csyteine couple could have a potential for electrochemical uses. Then their electrochemical reactions had been studied and it was seen that they

were activated strongly when an interaction occurred on the electrode surface. In this way, a new class of organic battery, which uses disulphide compounds (sulfur based redox dimerization and polymerization electrodes) as the cathode active material was illustrated in Japanese by Visco *et al* [47-55]. Chemical structures of organosulphur redox polymers are seen in Fig. 2.4.

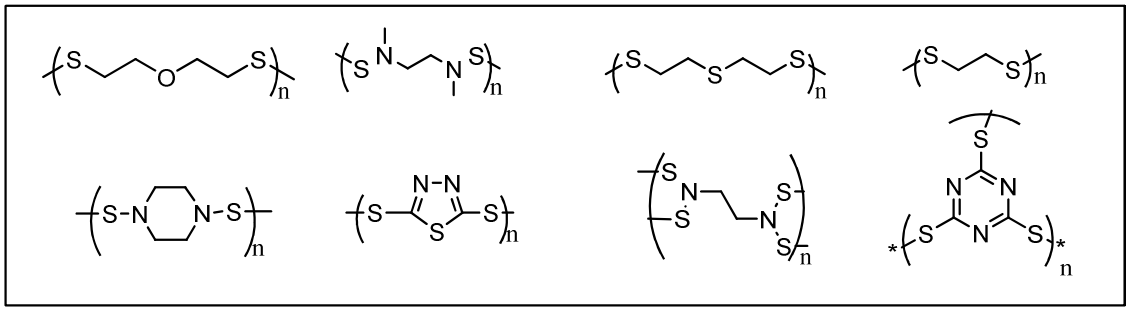

Figure 2.4. Chemical structures of organosulphur redox polymers.

In that years, tetraethylthiuram disulfide (TETD), diphenyl disulfide (PDS), and other organosulfur compounds were proposed as cathode-active materials, in conjunction with lithium or sodium anode. In such “redox polymerization electrodes”, the bonding and dissociation state of the (–S–S–) is used. Since bond-breaking and bond-formation of the covalent bond (–S–S–) process require the high activation overpotential, it causes slow electrode process [56-58].

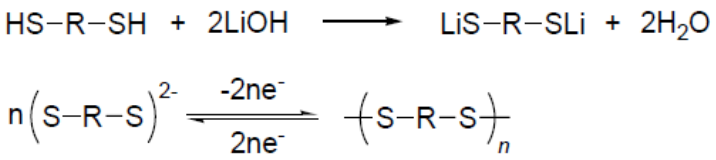

Scheme 2.1. Reaction mechanism of polydisulphide battery system.

Although these batteries with disulphide compounds show large theoretical capacity, this capacity decreases after a few charge-discharge cycles. And kinetically, slowness of the charge-discharge speed resulting insufficient charge-discharge cycles is a significant problem. Due to this problem, sulphide batteries have not been put into practical use.

2.1.2. Π-CONJUGATED POLYMERS OR CONDUCTING POLYMERS

Organic derived electrode-active battery materials have been studied since the 1980s. After the discovery of virgin polyacetylene, $(CH)_x$ by Shirakawa *et al.*[59] MacDiarmid and Heeger extend its properties from insulating to semiconducting or conducting state by reversibly oxidizing and reducing it. In this way, the potential application of p- and n- type doping processes in polyacetylene to rechargeable batteries was realized. After that, other conducting polymers such as polyphenylene, polypyrrole, polythiophene and polyaniline have been proposed and investigated for charge storage materials. Figure 2.5 shows the chemical structures of π-conjugated conducting polymers. Among the others, polyacetylene is regarded as a "model" material, on one hand because of its bivalence (as a host, both for positive and for negative charge) and on the other hand because of the vast theoretical knowledge acquired by physicists.

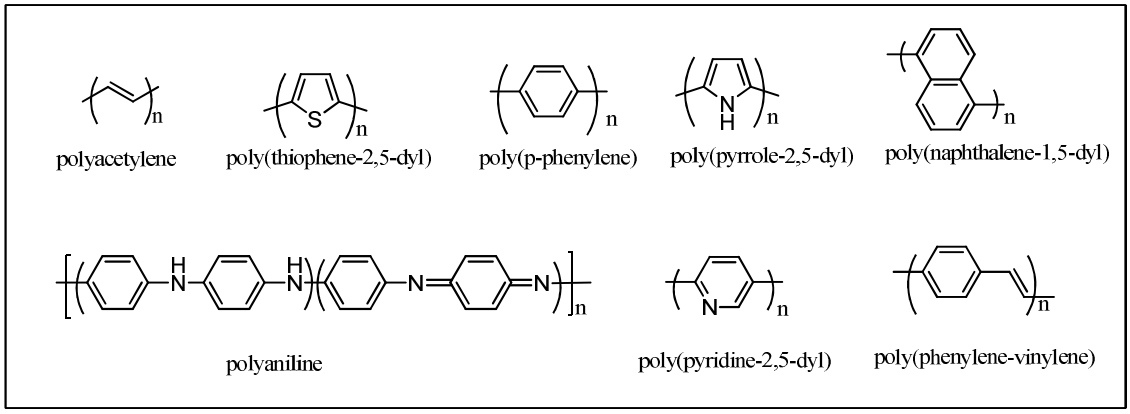

Figure 2.5. Chemical structures of π-conjugated conducting polymers.

It has to be emphasised that the conductivity strongly depends on the doping level of the polymer (redox state), which is formed during the cycling of the electrode. So, the proportion of the depth of charge-discharge is an important parameter for the determination of battery performance which is affected by the low ion mobility in the polymers and also in electrolyte system [60].

For the conducting polymers to be used as electrode active material, they must exhibit electrochemical and thermal stability during process and be stable in electrolyte solution. High doping amount per unit weight and unit volume, fast diffusion rate of dopant to the polymer molecules, fast oxidation and reduction (-reversibility of doping and undoping) and displaying high potential for p-type doping or low potential for n-

type doping are the most important parameters to consider the conducting polymers as active materials in battery applications. And of course, high conductivity is the desired property.

During their electrochemical oxidation and reduction, polymer electrodes must take up or give off ions in order to maintain electroneutrality of the material. This process is often called as polymer doping/undoping. The doping is an ion insertion process [61,62] that raises the redox state and electronic conductivity of the polymer. The charge-compensating ions can move within the polymer. Thus, a conducting polymer is actually an electronic as well as an ionic conductor.

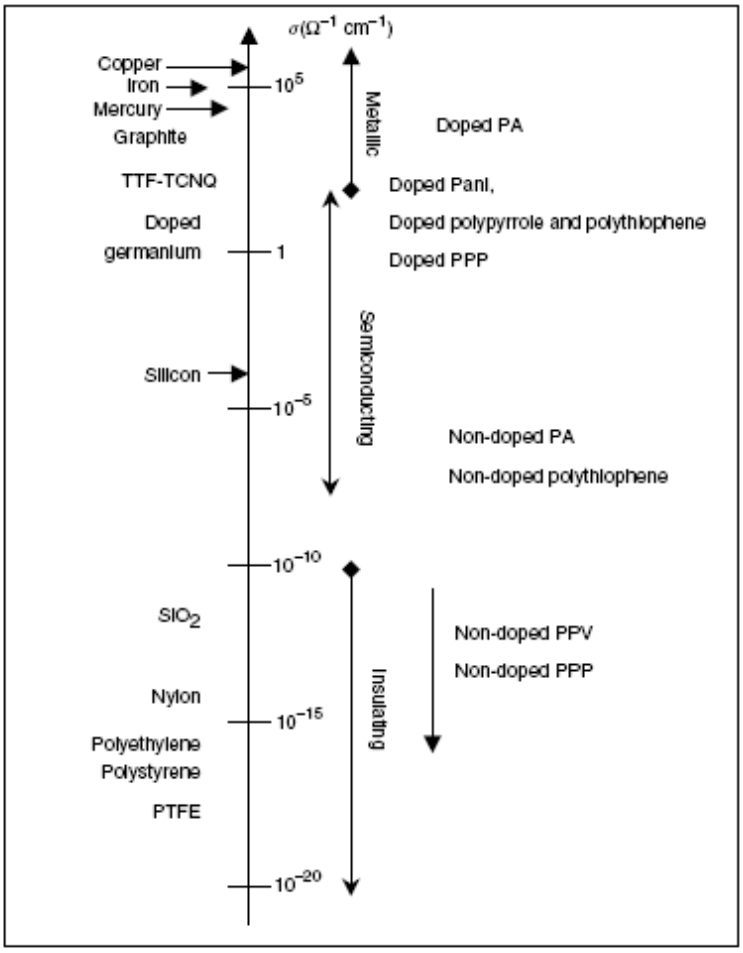

Figure 2.6. Conductivities of conjugated polymers compared with other materials [63].

Several doping procedures of polyacetylene were performed by MacDiarmid and co-workers [64]. Doping involves either oxidation or reduction of the polymer backbone. Oxidation removes electrons and produces a positively charged polymer and is described as ‘p-doping.’ Similarly, reduction produces a negatively charged backbone

and is known as ‘n-doping.’ These reactions can be done either by chemical species (e.g., iodine, sodium amalgam or sodium naphthaline) or electrochemically by attaching the polymer to an electrode. Polyacetylenes can be used as the anode or cathode, or both of them since it n- and p-dopes [65-69]. For the cathode, mostly ClO_4^- [70-72] and I^- [73] with BF_4^- [75], PF_6^- [76] and AsF_6^- [77,78] counterions are used to a lesser extent. Electrochemically doping the neutral polymer in an electrolyte solution, typically in propylene carbonate (PC) or tetrahydrofuran (THF), usually results in doping levels between 0.05 and 0.10 anions per repeat unit by using Li/Li^+ As a result, test cells can reliably obtain specific charge densities of 100–300 Ah/kg. The specific energy for PA-based electrodes ranges between 100 and 300 Wh/kg.

2.2. ORGANIC POLYMERS FOR RECHARGEABLE BATTERIES AND THEIR PERFORMANCE AS BATTERY ELECTRODES

Although conducting polymers are used in rechargeable batteries, they are not yet been widely available because of their low energy density. The low degree of doping concentration are the main reason for this problem. Since the doped electrons within the polymer are highly delocalized, and the large interaction between the charged electrons, which is called Coulomb repulsion, occurs. Therefore, it is difficult for conducting polymer-based batteries to increase the energy density. The electrode reaction of a conducting polymer-based rechargeable battery is shown in the Scheme 2.2.

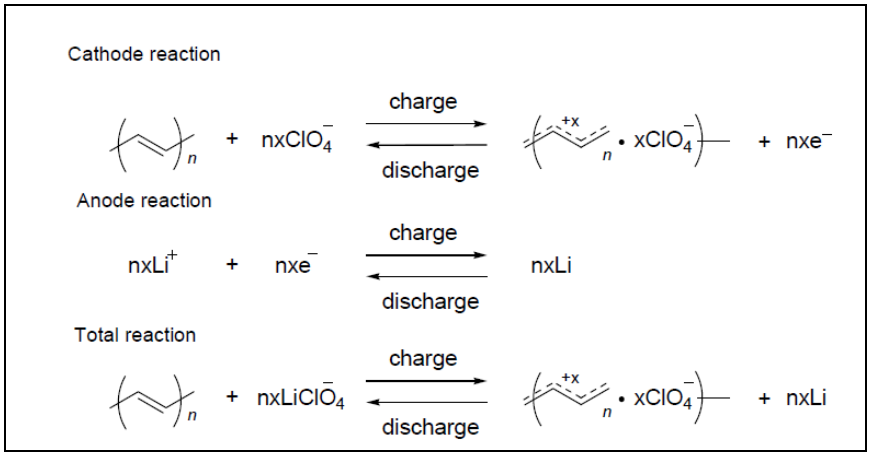

Scheme 2.2. Electrode reaction of rechargeable battery using polyacetylene [60].

2.2.1. IMPORTANCE OF NITROXIDE RADICAL

The nitroxide radical in TEMPO is characterized by its good chemical stability [79] depending on or coming from (or contributed by) its resonance structures. It shows two redox couples. On the anodic side, the nitroxide radical is oxidized to yield the corresponding oxoammonium cation (p-type doping) and on the cathodic side it is reduced to aminoxy anion leading to n-type doping of the material, as it is mentioned in part 2.1.

Oxygen centered nitroxide radicals have spin density localization on the oxygen atom and involves the resonance structure shown in Scheme 2.3.

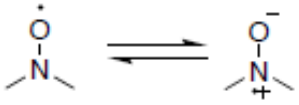

Scheme 2.3. Resonance structure for a nitroxide radical.

It is also characterized by its significantly small molecular weight per radical moiety (N-O = formula weight 30) and its compact molecular size. The anion in the electrolyte (eg. PF_6^- of $LiPF_6$ salt) takes part in the charge-discharge reaction at the radical cathode to keep the charge balance. During oxidation of nitroxide radical, an oxoammonium phosphorus hexafluoride salt is formed on the anodic side. On the cathodic side, the nitroxide radical is reduced to the aminoxy anion (e.g., the lithium alcoholate amine formation in $LiPF_6$), leading to n-type doping of the material. Therefore, organic radical polymers which are used as cathode active materials for lithium ion batteries are called as “organic radical batteries(ORBs)”.

Nakahara *et. al* of NEC Corporation, Japan first reported the application of the stable nitroxide radical-based material as the cathode for batteries [80]. They synthesized the polymer analogue of TEMPO, poly(2,2,6,6-tetramethylpiperidinyloxy methacrylate) (PTMA), studied its characteristics as the cathode for lithium battery and demonstrated its potential for realizing high-rate capable ORBs. Figure2.7 shows a prototype Li-ion battery with a polymer radical electrode on the anodic side and carbon electrode on cathodic side.

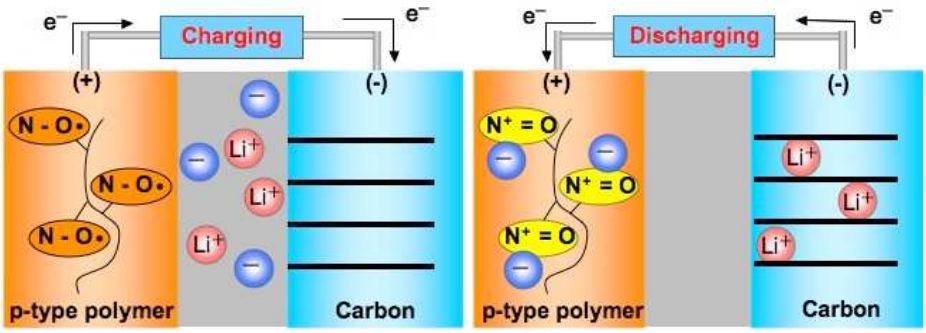

Figure 2.7. A lithium-ion battery based on a radical polymer cathode [21].

PTMA (chemical structure shown in Fig.2.3) is a derivative of polymethacrylate with TEMPO radical in its repeating unit. The synthesis procedures have been well reported. It can be synthesized by indirect method such as polymerization of 2,2,6,6-tetramethylpiperidine methacrylate followed by the oxidation reaction of the precursor polymer [79,81,82]. It is also prepared by the anionic polymerization of the radical monomer, 4-methacryloyl-2,2,6,6-tetramethylpiperidinyl-N-oxy. The former indirect synthetic method was resulted in incomplete oxidation of an amino group into a nitroxyl radical, resulting low radical concentration as charge storage material [80]. The synthetic routes are seen in the Scheme 2.4.

As a consequence, PTMA did not have the quantitative amount of radicals but approximately 70% against the theoretical value, and the batteries using this polymer showed an average discharge voltage of 3.5 V and a discharge capacity of 77 $Ahkg^{-1}$ (70% of the theoretical value).

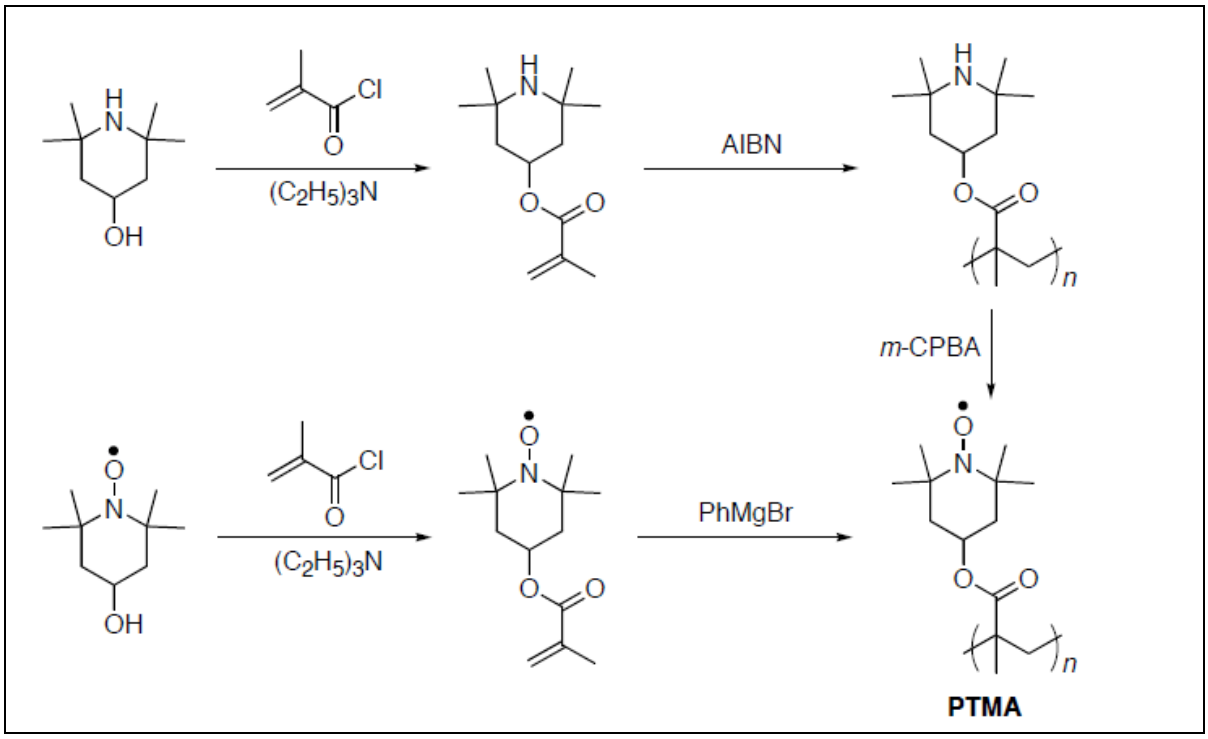

Scheme 2.4. Synthesis of poly(2,2,6,6-tetramethylpiperidinyloxy-4-yl methacrylate) (PTMA).

It has a molecular weight > 10000 and a glass transition temperature ~70°C. It is thermally stable up to ~250°C and the radical centers are stable up to the decomposition temperature of the polymer. It has already been demonstrated that under ambient conditions, the radical centers remain stable for more than a year. Since it is soluble in some of the organic solvents, it can be formed in thin sheets. Additionally, the insolubility of it in electrolyte solvents like diethyl carbonate (DEC), ethylene carbonate (EC) is a good property for a compound to be used as electrode materials.

Earlier studies showed that nitroxide radical exhibits fast electron transfer reaction. Its electron transfer constant k_0 is estimated using the Nicholson method to be approximately 10^{-1} cm.s^{-1}, about six orders faster than that of organic redox couples like disulphides [4]. This rapid electron transfer rate for the radical redoxes is the most important property when compared to the slow rates for the other organic redox reactions, for instance, the electron transfer rate constants of 10^{-4} and 10^{-8} cm.s^{-1} for the ascorbic acid oxidation and thional oxidation to form a disulphide respectively. The electron transfer reactions of radical molecules are rather faster than that of the ferrocene and are comparable to that for the copper ion [83].

So it is expected that ORB can display a quick charging and high power discharge capability due to this fast electron transfer rate. The main drawback for PTMA is lacking of molding ability and film forming ability. To solve this problem, photocrosslinking was preferred and in this way the solubility of the polymer was tuned and the mechanical toughness of the film was decreased [84]. And insufficient radical concentration of PTMA as charge-storage materials lead researchers to discover different materials. Nishide and Masuda independently performed the preparation and charge/discharge properties of several polyacetylenes and polynorbornenes containing TEMPO groups as a preliminary study and revealed that there are no polymers that exceed the capacity of PTMA [85-88]. They attempted to synthesize one or two TEMPO-substituted norbornene monomer and 7-oxanorbornene monomers and to polymerise these monomers ring opening metathesis (ROMP) method was used. A ruthenium-carbene catalyst which is referred to as “Grubbs 2nd generation” was applied [26]. The chemical structure of Grubbs 2nd-generation catalyst is shown in Figure 2.8 [85-90] and Scheme 2.5 shows the synthesis pathway of TEMPO-substituted polynorbornenes.

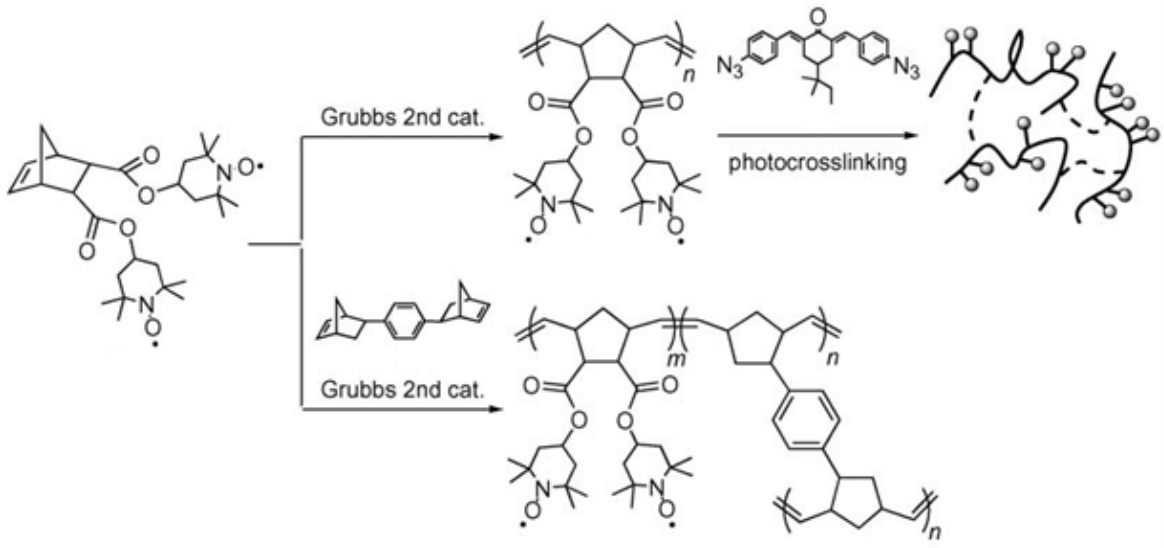

Scheme 2.5. Synthesis of the TEMPO-substituted polynorbornenes.

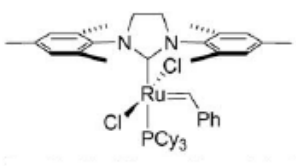

Figure 2.8. Chemical structure of Grubbs 2nd-generation catalyst.

Since these norbornone polymers displayed good solubility in common organic solvents, such as chloroform, ethyl lactate, and also in typical battery electrolytes, photocrosslinking was performed. It was done by forming radical polymer film on an indium tin oxide (ITO)/glass substrate. In that work, Nishide observed that ITO/glass substrate can be used as a new collector electrode for ORBs, because electron transfer from ITO to an organic radical polymer occurred without carbon. The cell performance of these material was also tested using a conventional size battery. The photocrosslinking process was applied after preparation of radical polymer-carbon composite. A test cell was fabricated by stacking the radical polymer–carbon composite cathode with a separator film and lithium metal as the anode. The specific capacity was 106 mAh/g, which agreed well with the theoretical capacity (109 mAh/g), calculated from the molecular weight of the radical moiety in the the polymer. The cycle performance during charging and discharging at the cut-off voltages of 3.0 and 4.2 V, respectively, displayed no significant deterioration in capacity up to 1000 cycles.
Since poly(7-oxanorbornene) did not display solubility problem like polynorbornenes, it can be applied to battery system accompanied with carbon fiber [88] the battery performance of some applied poly(7-oxanorbornene) derivatives versus Li electrode with a cell voltage range of 2.5–4.2 V demonstrated reversible charge/discharge processes with a discharge capacities up to 107 Ah/kg, respectively, corresponding to 98.3% of their theoretical capacity value. These cells also demonstrated excellent cycle life, e.g., the discharge capacities of some of their derivatives showed on the average of less than 10% decrements even after 100 cycles. These values are comparable to those of the reported PTMA system.

Masuda and Katsumata reported synthesis of TEMPO or PROXY–carrying polyacetylenes by direct polymerization of TEMPO containing acetylenes with a rhodium-based transition metal catalyst as it is seen in Scheme 2.6. For the polymerization of ester or amide containing these acetylene monomers $(nbd)^{+}Rh[\eta^{6}\text{-}C_6H_5B^{-}(C_6H_5)_3]$ or $[Rh(NBD)Cl]_2/Et_3N$ catalyst systems were used and moderate molecular weights was obtained in good yields. Radical containing these polymers displayed reversible charge/discharge processes, whose capacities almost reached to the therotical ones except TEMPO containing propargylester polymer. A coin type cell was fabricated by stacking the radical polymer–carbon composite cathode with a separator film and lithium metal as the anode.

They showed discharge capacity in the range of 43-112 mAh/g at a voltage range of 2.5-4.2 V. Large majority of them showed a promising cycle life, that is, the capacity hardly deterioriated even after 100 cycles. The polymers having one-handed helical structure exhibited higher capacity and tolerance to increase of current densities than non-helical polymers. This is an important property for polyacetylenes because introduction of helical structure was proved to be effective to enhance the battery performance. Some of the polymers displayed gradually a reduction in the charge and discharge capacites when current densities increase, presumably due to the polarization of TEMPO and PROXYL. Although some of them showed excellent properties, the capacities of polyacetylenes are stil lower than that of PTMA (111 mAh/g).

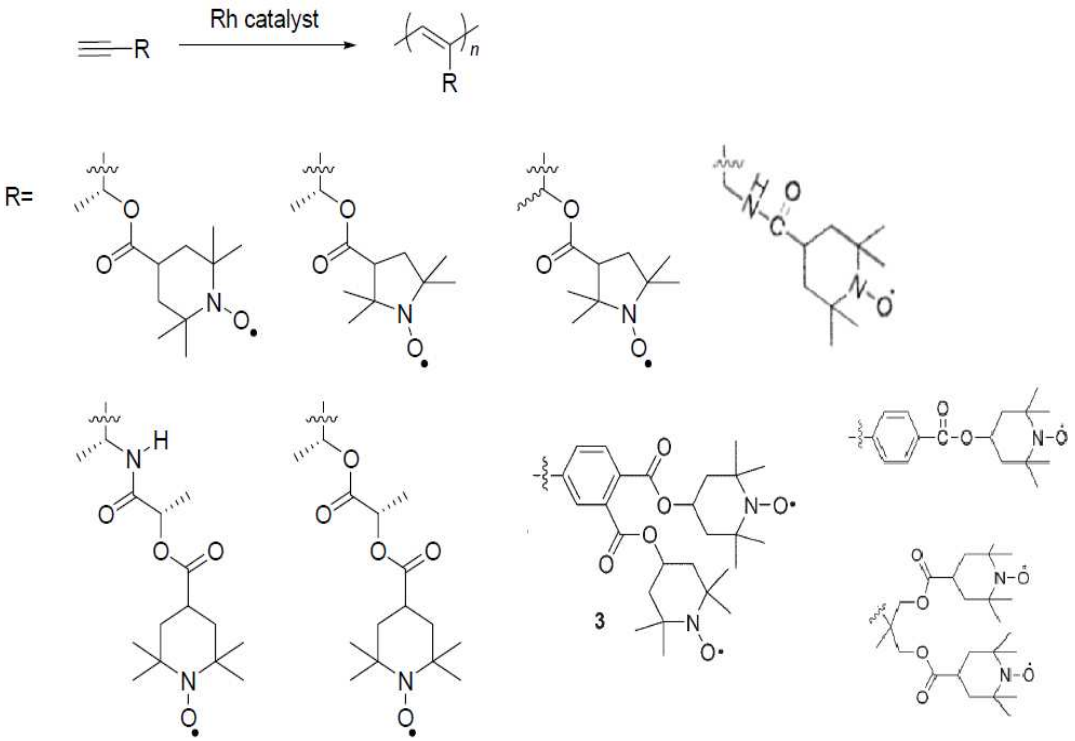

Scheme 2.6. Structures of synthesized polyacetylenes bearing TEMPO and PROXYL radical.

More recently, Masuda reported TEMPO-containing cellulose derivatives [91] and DNA–cationic lipid complexes [92] as the positive electrode material of ORB and found that they displayed two-stage discharge process. The total capacity of one TEMPO-containing DNA–cationic lipid complex reached 192% of the theoretical value

for one electron redox reaction, suggesting two-electron redox reactions between the cation and the anion. Although it sounds interesting, the actual capacity is lower than that of PTMA and are far from practical.

CHAPTER 3

EXPERIMENTAL PART

3.1. CHEMICALS

All organic reactions were performed under argon and dry N_2 atmosphere, and all chemicals were purchased and used as supplied without further purification unless otherwise is stated. Solvents used for reactions were distilled before use according to the standard procedures. Microporous film separator (#2400) were donated by Celgrad Inc.

3.2. MEASUREMENTS

Spin count and Magnetization Measurements

ESR studies were done on a BRUKER EMX series spectrometer designed for measurements in the X-band (9.5 GHz). ESR nitrogen hyperfine values were obtained via simulations performed using WinSim2002 program by Bruker.

The polymers were characterized by the g-value (2.0065) of the ESR signal which was same with that of TEMPO. The radical concentrations were determined by ESR spin count method, supposing that the polymers were paramagnetic at room temperature. Doubly integrated ESR nitroxide peak of the polymer under study was compared with that of the TEMPO as the standard. The radical concentration was also determined from the slope of the Curie plots (magnetic susceptibility (χ) vs temperature graphs) and magnetic data were corrected for the diamagnetic contribution of the sample holder. The 5–300 K magnetization measurements were carried out on a Quantum Design PPMS system under the constant magnetic field of 0.5kOe.

Electrochemical Measurements

Cyclic voltammograms were obtained with a potentiostat CHI instrument Model 842B. A platinum disk, platinum wire, and Ag/AgCl were used as the working, auxiliary, and reference electrode, respectively. The cyclic voltammogram was measured in an acetonitrile solution in the presence of 0.1 M tetrabutylammonium perchlorate as the supporting electrolyte.

Charge/discharge properties were measured at 25 ºC using a computer controlled automatic battery analyzer (BTS-8MA/5V/0.1-10mA) at different charge-discharge rates .

Chemical Characterization

^{1}H NMR and ^{13}C NMR were recorded using Bruker Ultra Shield Plus, Ultra long hold time 400MHz NMR Spectrometer. NMR spectra of radicals were taken after reducing them in the NMR tube by adding a few drops of phenylhydrazine. IR(ATR) spectra were recorded on Perkin Elmer BX-II FT-IR spectrometer equipped with diamond ATR kit in the range of 600-4000 cm^{-1}.

GPC measurements were performed on tetrahydrofuran (THF) solutions of the polymers (on the THF soluble parts of the polymer at a flow rate of 0.400 ml/min at 23°C using) using a Agilent GPC 1100 instrument. The measurements were standardized against THF solutions of a polystyrene standard.

Elemental analysis data was recorded by Thermo Scientific (CHNS analyzer), Flash 2000 instrument.

Morphological examinations of the composite materials were determined by using a Philips XL30 SFEG scanning electron microscope (SEM).

The thermal stability was determined by thermogravimetric analysis (TGA) on a STA 6000 model Perkin Elmer Instruments). The TGA thermograms were recorded for ca. 5 mg of powder sample at a heating rate of 10 ^{o}C/min in the temperature range of 30^{o}C-800^{o}C under nitrogen atmosphere**.**

The alternating current (AC) conductivities as a function of temperature of the polymer samples were measured using a Novocontrol dielectric-impedance analyzer in the frequency range from 0.1 Hz to 3 MHz. The samples with a diameter of 10 mm and a thickness of approximately 0.5 mm were sandwiched between two gold-coated

electrodes and their conductivities were measured at 10 K intervals under a dry nitrogen atmosphere.

Mass spectrometric measurements were recorded on a MICROMASS ULTIMA API spectrometer.

The glass transition temperature of the polymers was determined by Differential Scanning Calorimetry (DSC) analysis by using a Perkin Elmer Pyris 1 instrument at a heating rate of 10°C/min under a nitrogen flow.

UV–Vis measurements were carried out with Unicam double-beam spectrophotometer. Stock solutions of the monomers and polymers (only the soluble part in the solvent) were prepared by dissolving a few milligrams of the solid in 1-2 mL $CHCl_3$. These stock solutions were diluted if necessary.

3.3. CHEMICAL SYNTHESIS

3.3.1. Synthesis of Monomers

Monomers were synthesized according to the literature methods [93,94,96,97].

3.3.1.1. Synthesis of 1-oxyl-2,2,6,6-tetramethylpiperidin-4-yl-pent-4-ynoate Monomer (1)

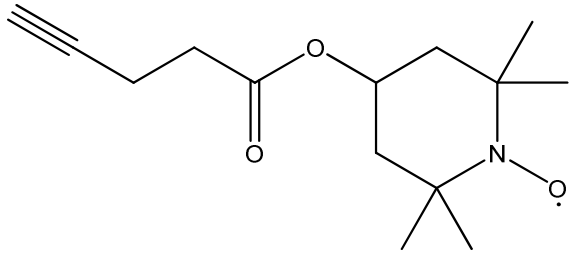

Figure 3.1. Structure of monomer (1).

This monomer was synthesized according to the reported procedure [95]. 4-pentynoic acid (500 mg, 5.097 mmol, 1.2 eq.) was added to a solution of EDCI•HCl (1.303g, 6.796 mmol, 1.6 eq.) and 4-dimethylaminopyridine (83 mg, 0.680 mmol, 0.16 eq.) in dry CH_2Cl_2 at room temperature under N_2(g). 4-hydroxy-TEMPO (730 mg, 4.247 mmol, 1 eq.) was added to the solution, and the resulting mixture was stirred at room temperature overnight. The precipitate was filtered and the reaction mixture was washed with water (80 mL) four times, and then brine. Finally the organic layer was dried over anhydrous $MgSO_4$. After filtration, the solvent was removed to afford a crude product which was then purified by column chromatography (silica gel, 5:1→ 7:3 hexane/ethyl acetate) to yield a dark orange solid (79% yield) whose color was due to the TEMPO radical. M.p. 51-53.9°C.

IR (ATR, cm^{-1}): 3234 $\upsilon_{(H-C\equiv)}$, 2997, 2974, 2932 $\upsilon_{(C-H)}$, 2117 $\upsilon_{(C\equiv C)}$, 1726 $\upsilon_{(C=O)}$, 1692, 1466, 1437, 1366 $\upsilon_{(N-O,\ radical)}$, 1352, 1310 ,1292, 1241, 1182, 1165 $\upsilon_{(C-O)}$, 1091, 1051, 1003, 978, 958, 893, 710, 682.

δ_H (400 MHz, $CDCl_3$): 1.8(s, 1H), 1.8-1.89, 1.5-1.55(t, 4H), 2.4(m, 4H), 5(m, 1H), 1.11, 1.13(d, 12H).

Elemental Analysis: Calcd for $C_{14}H_{22}NO_3$: C, 66.68; H, 8.79; N, 5.55. Found: C, 65.80; H, 8.79; N, 5.46. MS m/z = 235 [M^+]. (Theoretical m/z value = 236.16)

ESR ($CHCl_3$) analysis. 3 peaks at around g=2.0065 with nitrogen hyperfine value (A_N) of 15.429 G.

3.3.1.2. Synthesis of 1-oxyl-2,2,6,6-tetramethylpiperidin-4-yl-hex-5-ynoate Monomer (2)

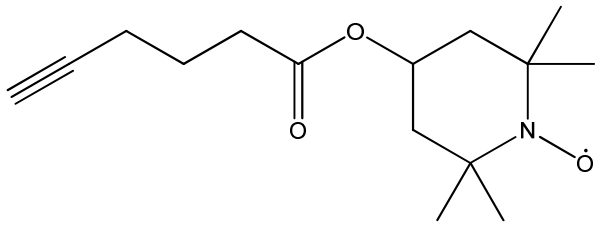

Figure 3.2. Structure of monomer (2).

This monomer was synthesized from 5-hexynoic acid and 4-hydroxy-TEMPO in a manner similar to monomer (2). It was purified by column chromatography (silica gel, 7:3 hexane/ethyl acetate) to yield a brownish liquid. Yield 78%.

FT-IR (cm^{-1}, in CCl_4): 3314 υ($_{H-C\equiv}$), 2975, 2934 υ($_{C-H}$), 2117 υ($_{C\equiv C}$), 1736 υ($_{C=O}$).

IR (ATR, cm^{-1}): 3282 υ($_{H-C\equiv}$), 2974, 2937, 2864, 2117 υ($_{C\equiv C}$), 1731 υ($_{C=O}$), 1462, 1363 υ($_{N-O,\ radical}$), 1315, 1238, 1156 υ($_{C-O}$), 1045, 1014, 984, 632.

δ_H (400 MHz, $CDCl_3$): 1.9(s, 1H), 1.84-.19, 1.53-1.59(2t, 4H), 2.3(t, 2H), 1.75(m, 2H), 2.1(t, 2H), 4.9(m, 1H), 1.14, 1.17(d, 12H).

Elemental Analysis: Calcd for $C_{15}H_{24}NO_3$: C, 67.64; H, 9.08; N, 5.26. Found: C, 58.69; H, 8.27; N, 3.95.

3.3.1.3. Synthesis of 4-propargyloxyl-TEMPO Monomer (3)

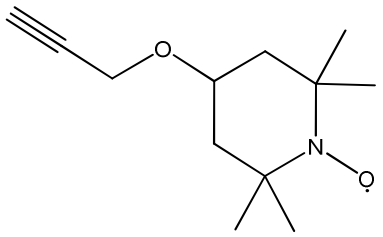

Figure 3.3. Structure of monomer (3).

This monomer was synthesized by applying two previously reported procedures [96,95]. To a stirring a suspension of NaH (60% in mineral oil, 170 mg, 4.180 mmol) in dry DMF (4 mL) 4-hydroxy-TEMPO solution (0.6 g, 3.480 mmol in 4 mL DMF) was added dropwise at 0ºC under N_2(g) and stirred at room temperature until gas evolution ceased (nearly~50 min). Propargyl bromide (0.539 g, 4.530 mmol) was added dropwise at 0ºC over a period of 45 min. The resulting mixture was allowed to warm up to room temperature and stirred overnight. The reaction mixture was quenched with ice water and the aqueous phase was extracted with ethyl acetate (4×25 mL) and the combined organic extracts were washed brine (2×30 mL), dried over $MgSO_4$, concentrated and dried under vacuum. The product was purified using column chromatography (silica gel, hexane → 2:1 hexane/ethyl acetate) to yield a dark orange solid (62.7% yield). Its color was attributable to TEMPO radical. M.p. 63.6-64.8°C.

IR(ATR) cm^{-1}: 3229 $\upsilon_{(H-C=)}$, 2996, 2973, 2936 $\upsilon_{(C-H)}$, 2111 $\upsilon_{(C\equiv C)}$, 1466, 1444, 1378, 1365 $\upsilon_{(N-O,\ radical)}$, 1347, 1175, 1082 $\upsilon_{(C-O)}$, 1021, 733, 691, 679.

Elemental Analysis: Calcd for $C_{12}H_{20}NO_2$: C, 68.54; H, 9.59; N, 6.66. Found: C, 68.06 H, 9.61; N, 6.40. MS m/z = 196 [M^+-16+2]. (Theoretical m/z value = 210.15)

δ_H (400 MHz, $CDCl_3$): 2.33(t, 1H), 4.05,4.06(d, 2H), 3.73(p, 1H), 1.83-1.87(q, 2H), 1.37(t, 2H), 1.11, 1.07(d, 12H). δ_C (400 MHz, $CDCl_3$): 20.523, 31.888, 44.249, 55.184, 69.685, 74.056. To obtain NMR spectra a few drops of phenyl hydrazine were added to NMR tube and in this way the radicals were reduced to corresponding hydroxylamine derivatives.

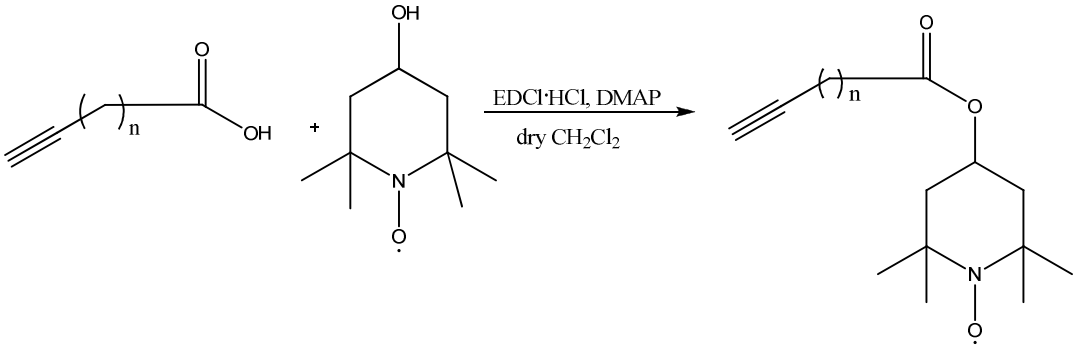

Scheme 3.1. Synthesis pathway of monomer (1), n=2 and monomer(2), n=3.

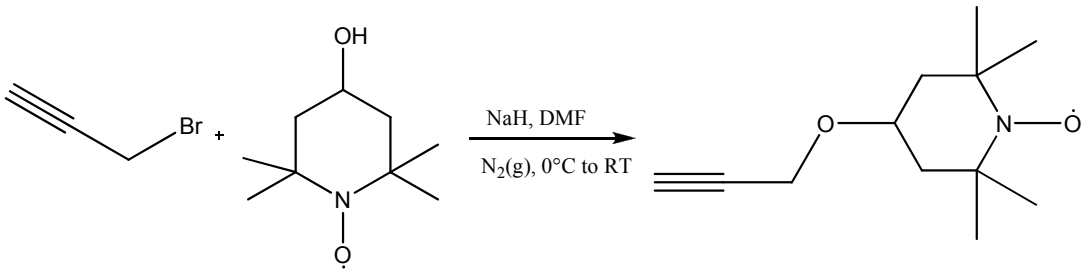

Scheme 3.2. Synthesis pathway of monomer (3).

3.3.2. Synthesis of Polymers

Polymerization of acetylenic monomers (1)-(3) were carried out using $[Rh(nbd)Cl]_2$ with cocatalysts such as Et_3N and LDA in different molar ratios. All polymerizations reactions were carried out under Ar(g) and dried glassware (all glassware were dried at 130°C at least for 40 min., then they were taken to desicator and cooled to room temperature under vacuum). The typical polymerization method mentioned below was applied in general just by changing solvent system, cocatalyst and concentrations of reactants in particular instances. The standard procedure is as follows: A THF solution (2.38 mL) of monomer (0.3 g, 1.190 mmol) and cocatalyst (0.481 mg, 4.759 µmol) was purged with Ar(g) and heated to 35ºC. A solution of $[Rh(nbd)Cl]_2$ (2.19 mg, 4.759 µmol) in THF was added with a syringe to the monomer/cocatalyst solution through a septum. The polymerization reaction was stirred overnight at 35°C, then it was poured into a large amount of *n*-hexane to give dark or light brown polymer precipitate. The precipitate was collected by centrifuging the suspension and removal of the supernatant liquid. The precipitate was washed with hot *n*-hexane using a soxhlet aparatus to remove any formation of impurities and unreacted monomer, and then dried under vacuum to constant weight.

Polymerization of acetylenic monomer (1) was also carried out by using ionic $[Rh(NBD)BF_4]$ catalyst in dry toluene and $CHCl_3$ mixture at 35ºC during overnight.
A solution of $[Rh(NBD)BF_4]$ (5.19 mg, 14 µmol) was prepared in a mixture of 3 mL of $CHCl_3$ and 1 mL toluene. Then, monomer solution (0.35 g, 1.39 mmol in 1.5 mL $CHCl_3$) was added to catalyst solution. [monomer]=0.25 M and [catalyst]=2.5mM.
After polymerization, the resultant solution was poured into large amount of methanol, diethylether or *n*-hexane to precipitate the formed polymer. The precipitate was collected by centrifuging the suspension and removal of the supernatant liquid. The

precipitate was washed with hot solvent to remove any formation of impurities and unreacted monomer, and then dried under vacuum to constant weight

IR(ATR) Data of the Polymers

Poly(1): 2974, 2937 $\upsilon_{(C-H)}$, 1730 $\upsilon_{(C=O)}$, 1596 $\upsilon_{(C=C)}$, 1463, 1363 $\upsilon_{(N-O,\ radical)}$, 1239, 1161$\upsilon_{(C-O)}$, 1085, 983, 873, 737, 682.

Poly(2): 3284, 2973, 2936 $\upsilon_{(C-H)}$, 1731 $\upsilon_{(C=O)}$, 1578 $\upsilon_{(C=C)}$, 1427, 1364 $\upsilon_{(N-O,\ radical)}$, 1310, 1238, 1164 $\upsilon_{(C-O)}$, 1011, 866, 750, 633.

Poly(3): 2974, 2933 $\upsilon_{(C-H)}$, 1653 $\upsilon_{(C=C)}$, 1462, 1360 $\upsilon_{(N-O,\ radical)}$, 1242, 1217, 1175, 1079 $\upsilon_{(C-O)}$, 900, 842, 683.

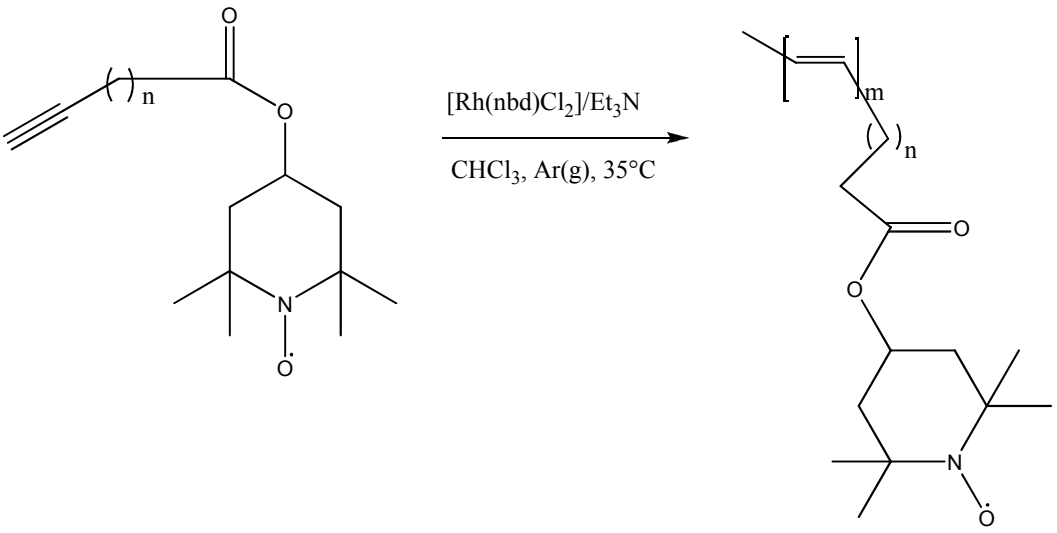

Scheme 3.3. Synthesis pathway of poly(1) and poly(2).

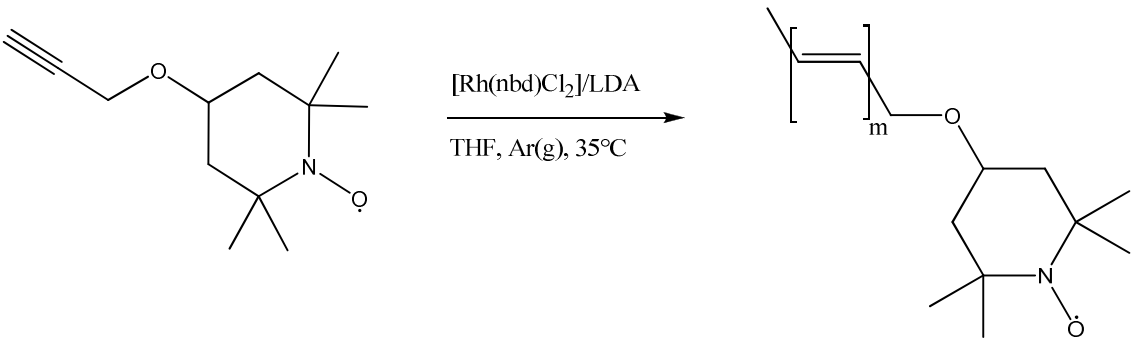

Scheme 3.4. Synthesis pathway of poly(3).

3.4. PREPARATION OF THE COMPOSITE ELECTRODE AND FABRICATION OF THE BATTERIES

The polymer (20 mg) was mixed with 70 mg of a graphite fiber and 10 mg of a binder powder (polyvinylidenefluoride resin) in the presence of N-methyl-2-pyrrolidone (NMP). The mixture was homogenized by blending with a ball milling system for an hour. Then it was pasted on aluminium foil (shaped as a disc 19 mm in diameter) and dried overnight in vacuum at 40ºC [85,86]. Thickness of cathodes was varied between 0.09 mm and 0.1 mm. The mass of active material on the cathode changes between 1.6 to 2.6 mg for these thicknesses. CR2016 type coin cell was used.

A coin type cell was fabricated by stacking the polymer/graphite composite electrode, porous polypropylene separator sheet (Celgrad #2400, Hochst Celanese Co., Ltd.), lithium metal or graphite sheet (MTI corporation 15 mm diameter on Cu foil, 0.2 mm thickness) as the anode and a stainless steel current collector under an argon atmosphere. An mixture of ethylene carbonate / diethylcarbonate (30:70 vol%) containing 1M of $LiPF_6$ was used as an electrolyte solution. Battery charge/discharge characteristics were evaluated by measurements performed at 25°C using a computer controlled battery charge-discharge instrument.

CHAPTER 4

RESULTS AND DISCUSSION

4.1. MONOMER SYNTHESIS

Acetylene ester monomers, namely 1-oxyl-2,2,6,6-tetramethylpiperidin-4-yl-pent-4-ynoate **(1)** and 1-oxyl-2,2,6,6-tetramethylpiperidin-4-yl-hex-5-ynoate **(2)** were synthesized by the condensation of the carboxyl group of 4-pentynoic acid or 5-hexynoic acid with the hydroxy group of 4-hydroxy TEMPO (4-hydroxy-2,2,6,6-tetramethylpiperidin-1-oxy). 4-propargyloxyl-TEMPO monomer **(3)** was synthesized by nucleophilic substitution reaction of propargyl bromide with sodium salt of 4-hydroxy-TEMPO prepared in situ by the action of sodium hydride on 4-hydroxy-TEMPO. The monomers were purified by silica gel column chromatography utilizing ethyl acetate/*n*-hexane(7/3 or 2/1 volume ratio) as eluent.

The structures of the monomers were confirmed by IR(ATR) and ^{1}H NMR spectroscopy. The presence of free radicals did not allow measuring the NMR spectra of the monomers. Hence, they were reduced to the corresponding hydroxylamine derivatives by adding a few drops of phenylhydrazine to the NMR tube containing $CDCl_3$ solution of the monomers [98,99]. Further confirmation for the structure of the monomers was furnished by elemental and mass spectral analysis gave very close results to the theoretically expected ones (see the Experimental Section).

4.1.1. Structural Characterization of Monomers

The IR(ATR) spectrum of synthesized monomer **(1)** is shown in Fig. 4.1. The characteristic peaks of sp C-H bond and carbon-carbon triple bond stretchings can be differentiated easily. So, the strectching vibrations of C≡C and H-C≡ at 2121 cm^{-1} and 3233 cm^{-1} proves the existence of acetylene in the monomer. Disappearance of broad H-O stretching peak resulting from carboxylic acid group of 4-pentynoic acid in the range of 2421-3192 cm^{-1} and shifting of carbonyl peak (C=O) of 4-pentynoic acid from 1692 cm^{-1} to 1724 cm^{-1} proves the conversion of acid functional group to the ester moiety. The presence of a peak at 1368 cm^{-1} assignable to the nitroxy radical also implies that TEMPO moiety is successfully bonded to acetylenic compound. By TLC monitoring the purity of the monomer was also tested. The structure of this monomer was also supported by ^{1}H NMR as it is seen in Fig. 4.2.

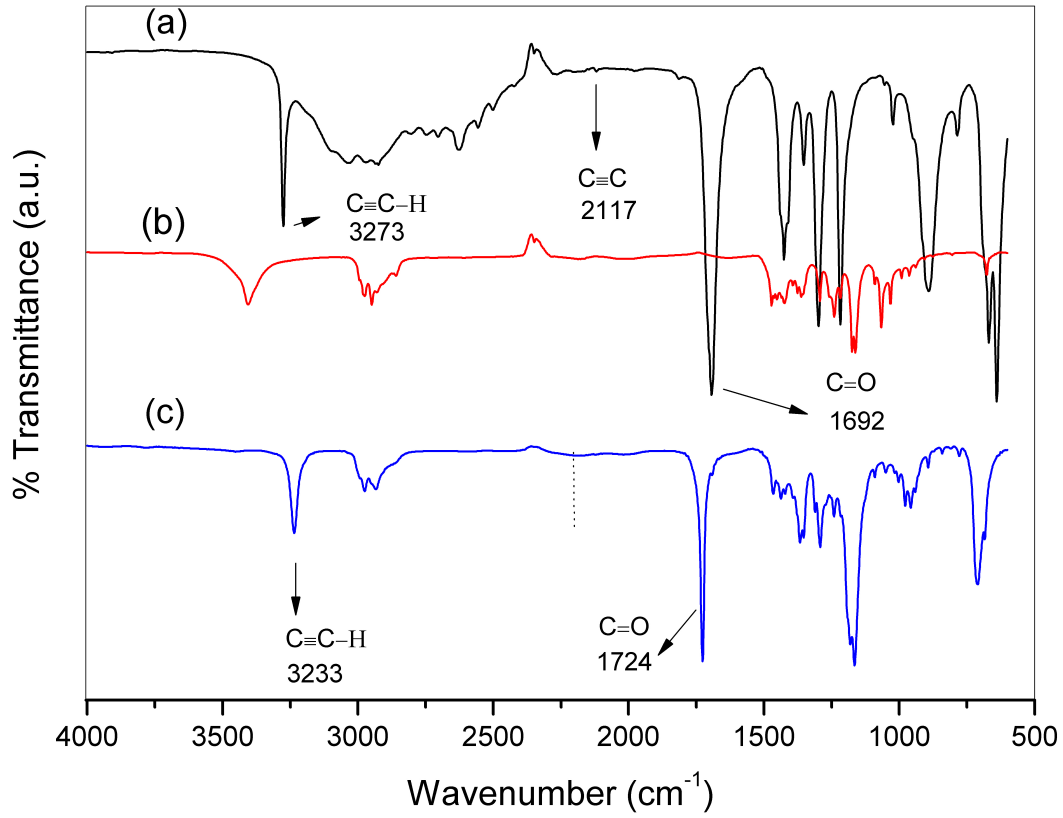

Figure 4.1. ATR spectrum of 4-pentynoic acid **(a)**, 4-hydroxy TEMPO **(b)**, monomer (1), 1-oxyl-2,2,6,6-tetramethylpiperidin-4-yl-pent-4-ynoate **(c).**

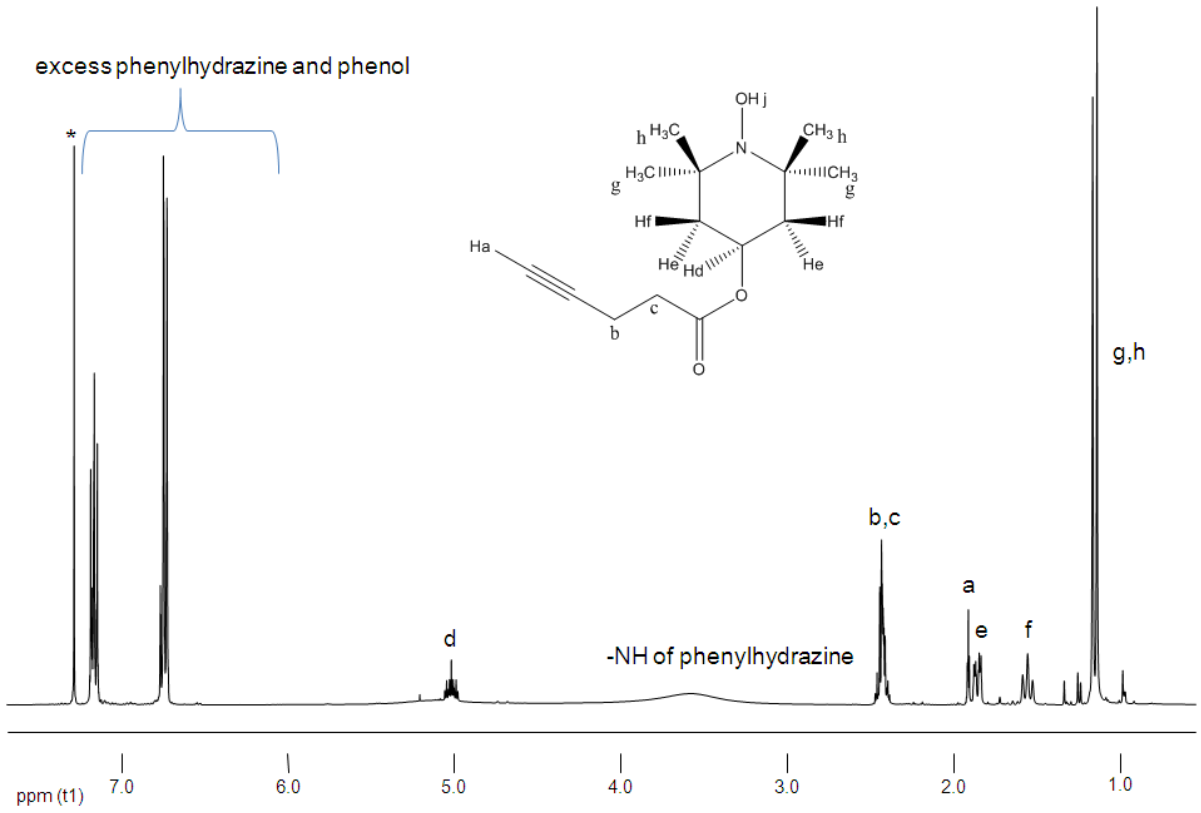

Figure 4.2. ^{1}H NMR spectrum of monomer (1), 1-oxyl-2,2,6,6-tetramethylpiperidin-4-yl-pent-4-ynoate in $CDCl_3$.

The signal of terminal acetylene proton (a) appeared at 1.8 ppm as triplet and overlapped with the (e) protons. Protons (e) and (f) which are bonded to on the same carbon give doublet of triplet at 1.8-1.89 and 1.5-1.55, respectively. The protons (b) and (c) were seen as multiplet at 2.4 ppm. The proton (d) was seen at 5 ppm as a multiplet. The protons (g) and (h) of tetramethyl groups of the TEMPO radical were observed as two different singlets at 1.11 and 1.13 ppm due to the their differing chemical environments. The excess phenylhydrazine signals were also seen at aromatic region between 6.7-7.2 ppm. The additional broad peak at 3.4 ppm belonges to amine of excess phenylhydrazine reagent. The correct integrations were obtained for all protons a(1H), b(2H), c(2H), d(1H), e(2H), f(2H),g(6H), h(6H).

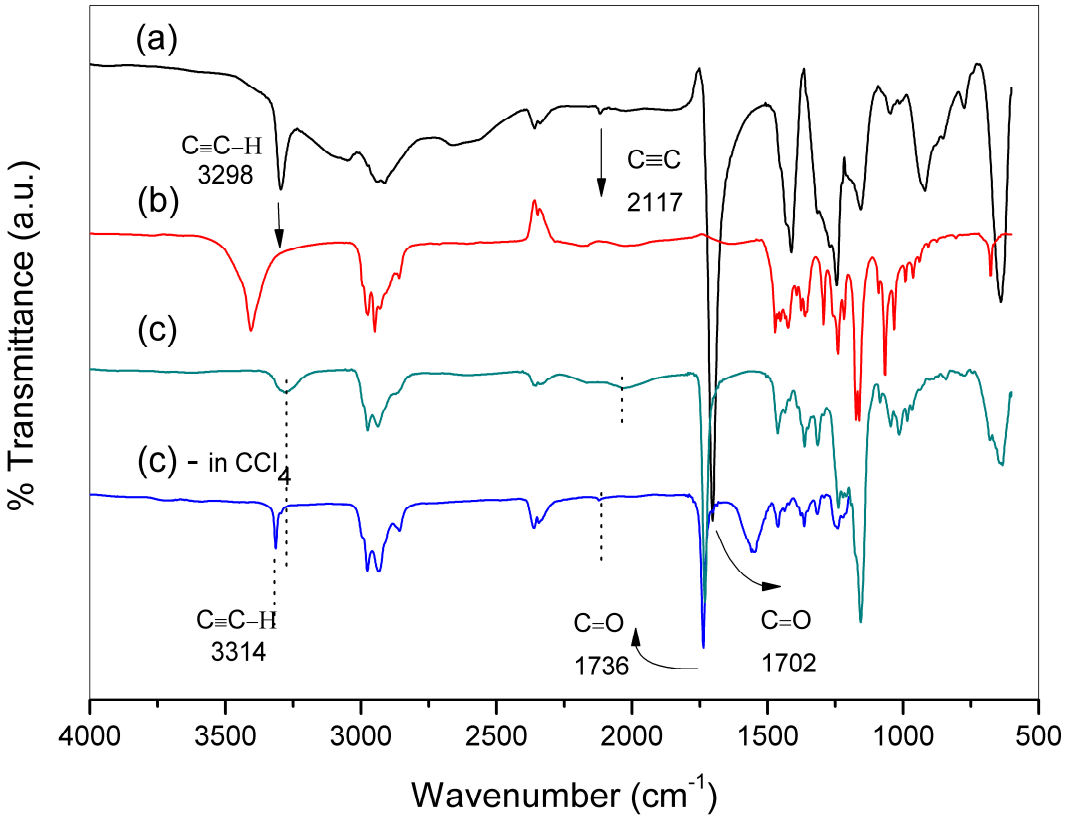

Figure 4.3. ATR spectrum of 5-hexynoic acid **(a)**, 4-hydroxy TEMPO **(b)**, monomer (2), 1-oxyl-2,2,6,6-tetramethylpiperidin-4-yl-hex-5-ynoate **(c)** and FT-IR spectrum of a solution of 1-oxyl-2,2,6,6-tetramethylpiperidin-4-yl-hex-5-ynoate **(c)** in CCl_4**.**

The chemical structure of 1-oxyl-2,2,6,6-tetramethylpiperidin-4-yl-hex-5-ynoate (monomer **(2)**) was confirmed by both IR (ATR) and ^{1}H-NMR spectroscopy. IR(ATR) spectrum of monomer **(2)** is given in Fig. 4.3. In monomer **(2),** the conversion from a carboxylic acid to an ester is indicated by the disappearance of broad O-H stretching peak of carboxylic acid between 2572-3054 cm^{-1} and shift of the carbonyl group (C=O) peak from 1702 cm^{-1} to 1730 cm^{-1} . The stretching vibration of sp C-H of acetylene shifted to 3314 cm^{-1} from 3295 cm^{-1}. And C-O stretching vibration is observed at 1156 cm^{-1}. Since IR (ATR) spectrum directly run on this monomer in the pure form (liquid) is not clear about the strectching vibrations sp C-H and C≡C of acetylene, the spectrum was taken again in CCl_4 solution of the monomer and the peaks before 1600 cm^{-1} is not

taken into consideration. sp C-H and C≡C stretching peaks of terminal acetylene group is more clearly observed in this form.

Monomer (2) was also reduced with phenyl hydrazineto N-hydroxyl amine (N-OH) and NMR spectrum and the assignment of the protons of this reduced monomer is shown in Figure 4.4.

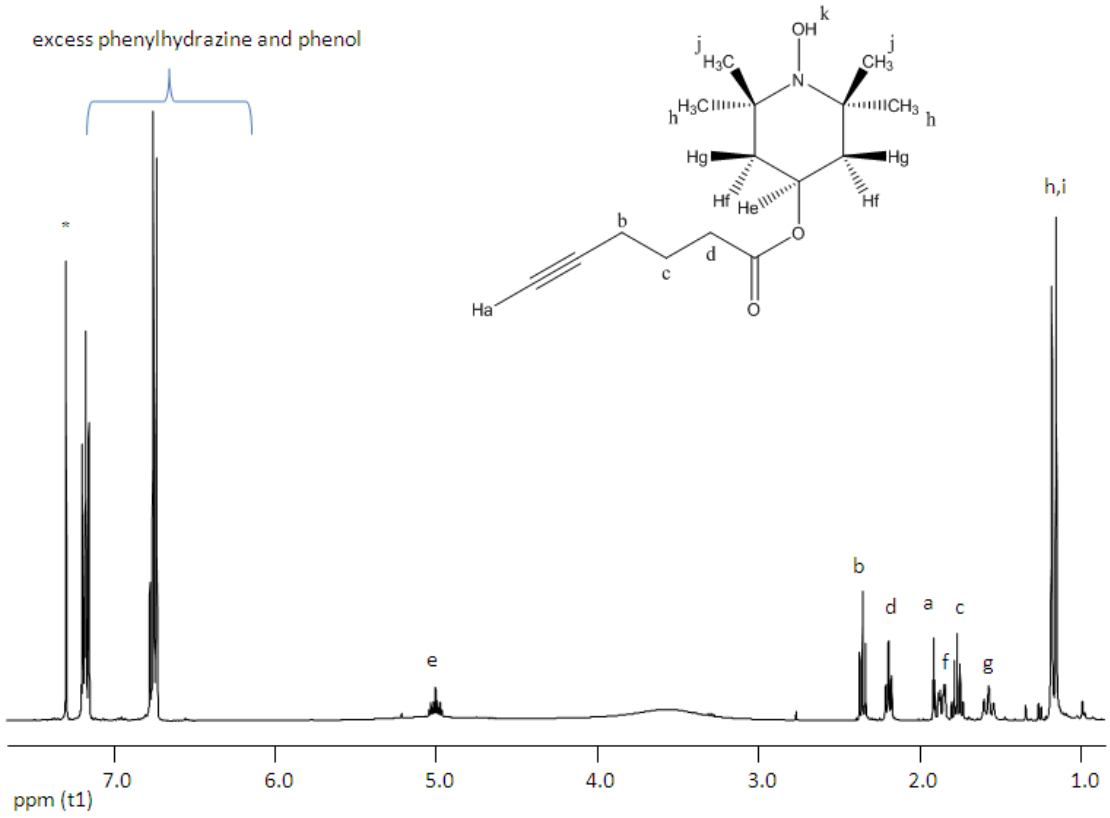

Figure 4.4. ^{1}H NMR spectrum of monomer (2), 1-oxyl-2,2,6,6-tetramethyltetramethylpiperidin-4-yl-hex-5-ynoate in $CDCl_3$.

The signal of terminal acetylene proton (a) appeared at 1.9 ppm as triplet and overlapped with the protons of f. Protons (f) and (g) which are bonded to on the same carbon give doublet of triplet at 1.84-1.9 and 1.59-1.53 ppm, respectively. The protons (b) were seen as triplet at 2.3 ppm. The protons (c) were seen as multiplet at 1.75 ppm. The protons (d) was seen as triplet at 2.1 ppm. The proton (e) was seen as multiplet at 4.9 ppm.

The protons (h) and (i) of tetramethyl groups of the TEMPO radical were observed as two different singlets at 1.14 and 1.17 ppm due to the their differing chemical environments. The excess phenylhydrazine signals were also seen at aromatic region

between 6.7-7.2 ppm. And additional broad peak at 3.4 ppm belonged to amine of excess phenylhydrazine reagent.

The correct integrations were obtained for all protons protons a(1H), b(2H), c(2H), d(2H), e(1H), f(2H),g(2H), h(6H), j(6H).

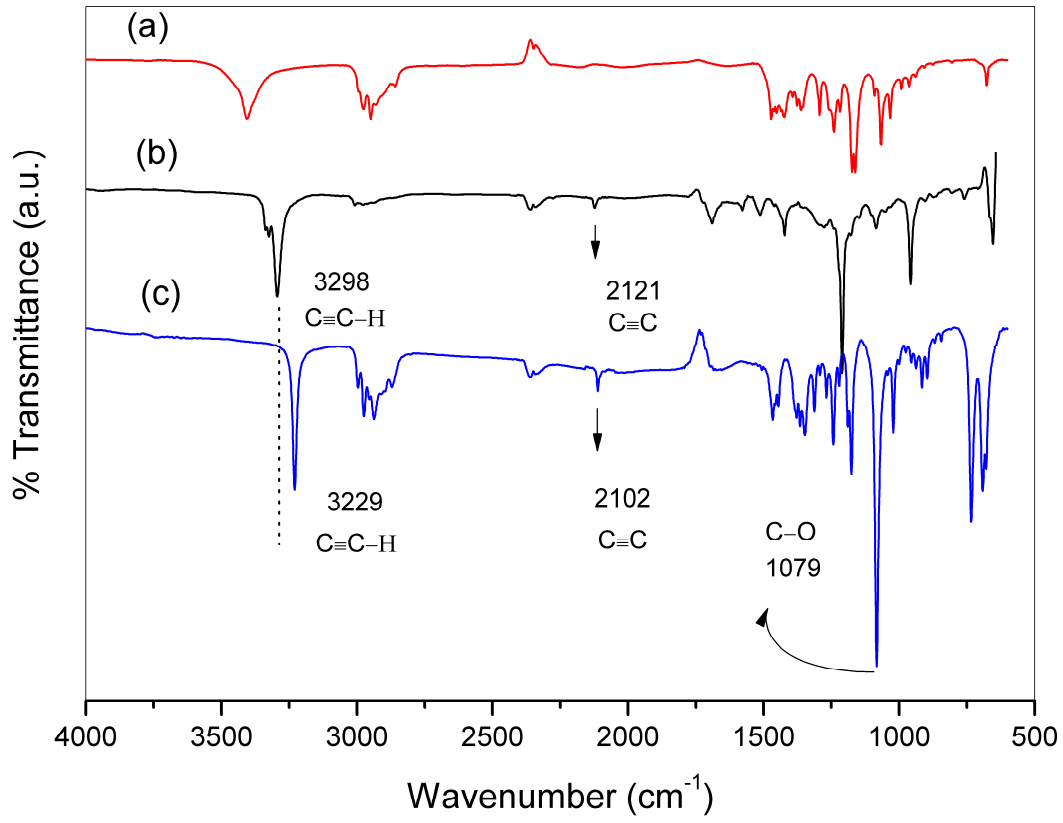

Figure 4.5. ATR spectrum of 4-hydroxy TEMPO **(a)**, propargyl bromide **(b)**, monomer (3), 4-propargyloxy-TEMPO **(c).**

The chemical structure of 4-propargyloxy-TEMPO (monomer **(3)**) was confirmed by both IR (ATR) and ^{1}H-NMR spectroscopy. The monomer was reduced by phenyl hydrazine as was mentioned previous sections prior to NMR analysis. The IR (ATR) spectrum shown in Figure 4.5 establishes the structure of the monomer **(3)**. In the spectra, a new peak's appearance at 1079 cm^{-1} proves the existence of the ether functional group in the monomer.

Accordingly, diagnostic stretching vibrations of terminal acetylenic C-H and C≡C bands appear at 3229 cm^{-1} and 2102 cm^{-1}, respectively. Moreover, the stretching vibrations of

sp^3 C-H and N-O around 2997-2868 cm^{-1} and 1360 cm^{-1} respectively prove that TEMPO moiety exist in the monomer.

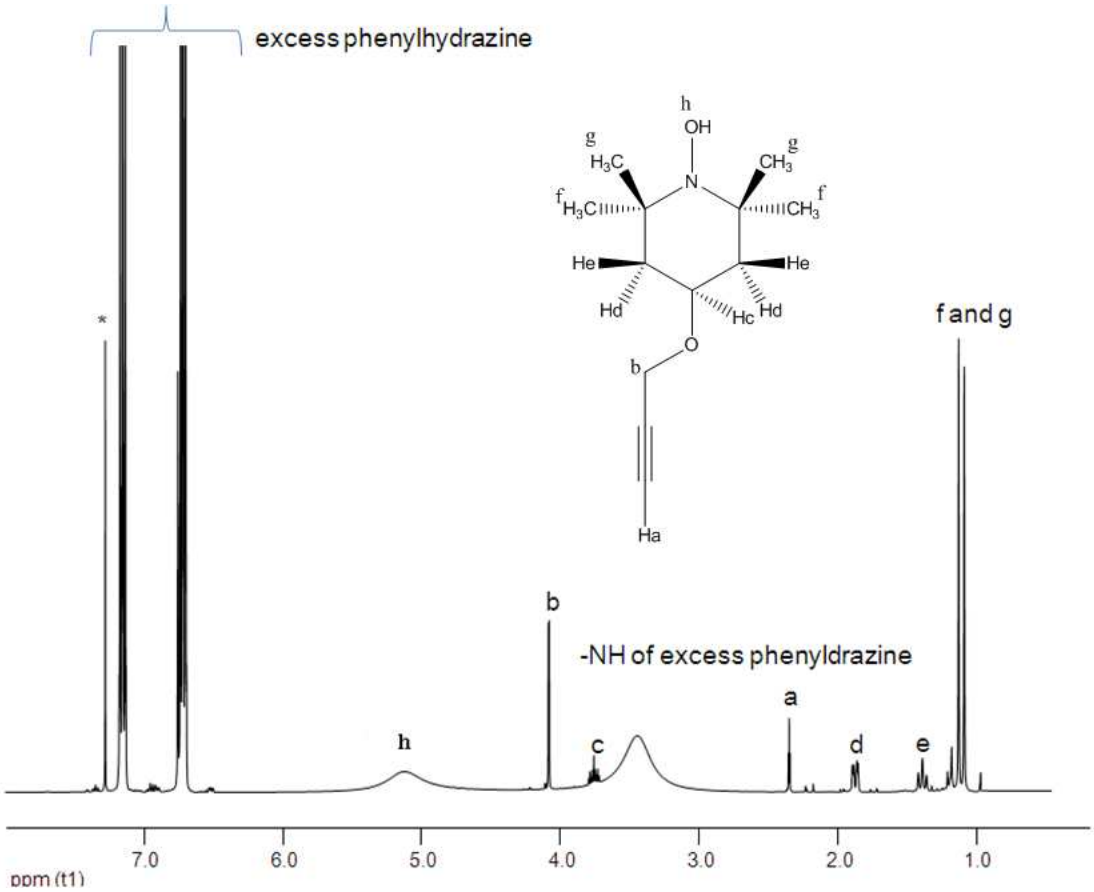

Figure 4.6. ^{1}H NMR spectrum of monomer (3), 4-propargyloxy-TEMPO in $CDCl_3$.

The structure of the 4-propargyloxy-TEMPO was also supported by ^{1}H NMR and ^{13}C NMR. ^{1}H NMR spectrum was seen in Fig. 4.6. and ^{13}C NMR was given in Appendix A. The signal of terminal acetylene proton (a) emerges as triplet at 2.33 ppm, two (b) protons of the propargyl part were seen as a singlet at 4.05 ppm. One proton on the C4 was seen as pentet at 3.73 ppm and protons (d) and (e) appeared as doublet of triplet at 1.83-1.87 ppm and at 1.372 ppm, respectively. The tetramethyl groups of the tempo radical were observed as singlets at 1.11 and 1.07 ppm. The excess phenylhydrazine signals were seen at aromatic region between 6.7-7.1 ppm. The broad peak at 5.1 ppm comes probably from N-O-H group. And additional broad peak at 3.4 ppm belonged to amine of excess phenylhydrazine reagent. All the asignments above were done by taking into consideration of the number of protons and NMR peak integration values.

4.2. Polymer Synthesis

The polymerization of acetylene monomers was carried out using $[Rh(nbd)Cl]_2$ catalyst with two different cocatalysts (Et_3N and LDA) in THF, $CHCl_3$ and toluene at 35ºC overnight. The results are summarized in Table 4.1.

Polymers were obtained as brown powders or as brownish brittle films in yields of 7-51% exhibiting M_n values between 625 and 381.400. Some of these polymers were soluble in THF and $CHCl_3$ and some of them were partially soluble in these solvents. All polymers were found to be insoluble in *n*-hexane. The differences in solubilities can not be simply attributed to choice of polymerization conditions because the sample history and polymer aggregation also play important role in determining the solubility of the polymers obtained. For example, when homogeneous polymer solutions were evaporated to dryness and tried to be redissolved in the same solvent, some part of the polymer became insoluble in the solvent due to aggregation or structural changes that may have occurred (cis-transoid, all transoid and or cisoid structures are possible when relative configurations of neighboring double bonds are considered) during evaporation since heating is applied.

When the effect of the type of cocatalyst used (Et_3N or LDA) was compared in reactions, there was no distinguishable result obtained on the molecular weight of polymers (run 9 vs run 10 on in Table 4.1). But, it should be noted that there was a small increase in the yield of polymerizations when LDA was used.

Using toluene in polymerization reactions provided a reaction medium giving polymers with a higher molecular weight (run 6 vs run 7).

The monomer concentration change showed no appreciable difference in polymer molecular weights (run 6 vs 10). Increasing the monomer concentration induced the formation of a polymer with slightly lower molecular weight, but with a significantly higher polymerization yield.

When [Cat]/[Cocat.] ratio was applied as 1/2 rather than 1/10, THF insoluble polymers with possibly high molecular weights were obtained with very low yields as seen for runs 4 and 5. As the [Cat]/[Cocat.] ratio was decreased to 1/10, the molecular weight of poly(1) decreased although a more soluble polymer with a higher yield is obtained (run 5 vs run 6).

Table 4.1. Polymerization of acetylenic monomers **(1) - (3)** with Rh Catalyst.

Run	Monomer	Catalyst	[M]	[M]/[Cat.]	[Cat]/[Cocat.]	Solvent	Yield (%)	Mn	PDI
1	1	$[Rh(nbd)Cl]_2$/TEA	0.2	50	1/100	$CHCl_3$	10[a)]	17 100	1.53
2	1	$[Rh(nbd)Cl]_2$/TEA	0.5	250	1/1	THF	9[d)]	7 177[c)]	1.103
3	1	$[Rh(nbd)Cl]_2$/LDA	1.25	250	1/1	toluene	21 [b)]	383700	1.331
4	1	$[Rh(nbd)Cl]_2$/LDA	0.5	250	1/2	toluene	5[a)]	---e	---e
							9[b)]	698.4	1.169
5	1	$[Rh(nbd)Cl]_2$/LDA	0.5	250	1/2	THF	7[a)]	---e	---e
							16[b)]	625[c)]	1.252
6	1	$[Rh(nbd)Cl]_2$/LDA	0.5	250	1/10	THF	33[b)]	942.2	1.688
7	1	$[Rh(nbd)Cl]_2$/LDA	0.5	250	1/10	Toluene	26 [b)]	351600	1.635
8	1	$[Rh(nbd)Cl]_2$/LDA	0.5	250	1/10	Toluene, 55°C	24 [b)]	323000	1.786
9	1	$[Rh(nbd)Cl]_2$/LDA	0.2	250	1/10	THF	9 [b)]	912.4	1.755
10	1	$[Rh(nbd)Cl]_2$/TEA	0.2	250	1/10	THF	7 [b)]	1317	1.461
11	1	$[Rh(nbd)Cl]_2$/LDA	0.5	200	1/1	THF	16 [b)]	336 900	1.543
12	1	$[Rh(nbd)Cl]_2$/LDA	0.2	100	1/10	THF	51[b)]	10 530[c)]	1.25
13	1	$[Rh(NBD)BF_4$	0.25	100	-----	$CHCl_3$+ toluene	34[b)]	855.6 [c)]	1.8
14	2	$[Rh(nbd)Cl]_2$/LDA	0.2	100	1/10	THF	16 [b)]	---e	---e
15	2	$[Rh(nbd)Cl]_2$/LDA	0.2	200	1/10	THF	9[b)]	265900[c)]	1.578
16	2	$[Rh(nbd)Cl]_2$/TEA	0.2	100	1/100	THF	9[b)]	340100	1.648
17	3	$[Rh(nbd)Cl]_2$/LDA	0.2	100	1/10	THF	29 [b)]	1055	1.2
18	3	$[Rh(nbd)Cl]_2$/TEA	0.2	50	1/100	$CHCl_3$	28 [b)]	381400	1.540
							36 [b)]	949.7	1.760

* a) MeOH insoluble part, b)Hexane insoluble part, c) THF soluble part (some of the polymers contain both THF soluble and insoluble part), d) Diethylether insoluble part, e) THF insoluble.

** All polymerizations were done at 35ºC, unless otherwise noted.

Interestingly, monomer to catalyst molar ratio ([M]/[Cat.]) is found to be the best when it is around 100. Lower polymer yields and molecular weights were obtained if this ratio is any lower or any higher than this value (run 9 vs 12 and run 14 vs 15).

A drastical yield increase (51%) with a simultaneous high molecular weight was observed (run 12) when 0.2 M monomer concentration with 2mM catalyst concentration were used. 62% of the obtained polymer were insoluble in THF, $CHCl_3$, CH_2Cl_2.

Polymerization with ionic catalyst also displayed good result as it was seen run 13. Due to solubility problem of catalyst toluene and $CHCl_3$ solvent mixture was used. 4.9% of obtained polymer was insoluble in THF. Interestingly, run 11 yielded brittle polymer in polymerization reactions of monomer (1).

Polymerization of monomer (1), (2), and (3) with same molar ratios displayed different results. Monomer (2) exhibited 100% THF insoluble polymer compared with monomer (1) and (3). This was probably because of one carbon number increment in polymer repeating unit. When runs 1 and 18 are compared with each other, we can see that [Cat]/[Cocat.] ratio of 50 worked better for the polymerization of monomer (3) than for polymerization of monomer (1). So far optimum conditions observed for polymerization of monomer (1) are 0.2 M monomer concentration, 2mM catalyst concentration, [catalyst]/[cocatalyst]=1/10, and THF solvent which gives an insoluble and high molecular weight polymer in 32% yield (hexane insoluble polymer yield obtained was even higher, 51%). Increasing the monomer concentration to 0.5 M may have yielded a higher yield.

4.2.1. Structural Characterization of Polymers

Figure 4.7, 4.8, and 4.9 show the ATR spectrum of polymers. Poly(1)-poly(3) exhibited no IR peaks at around 3270 and 2120 cm^{-1} that arise from stretching vibrations of sp C-H and C≡C respectively, thus indicating that acetylene polymerization took place. And a small absorption band occurrence at around 1580 cm^{-1} proves existence of conjugated double bond in the polymers. The IR(ATR) spectra of the polymers (1) and (2) show strong peaks at around 1730 and 1160 cm^{-1} assignable to C=O and C-O stretching vibrations thus implying ester group. All polymers exhibit a peak at around 1362 cm^{-1} stemming from nitroxy radical N-O bond which proves that TEMPO moiety is present in the polymers.

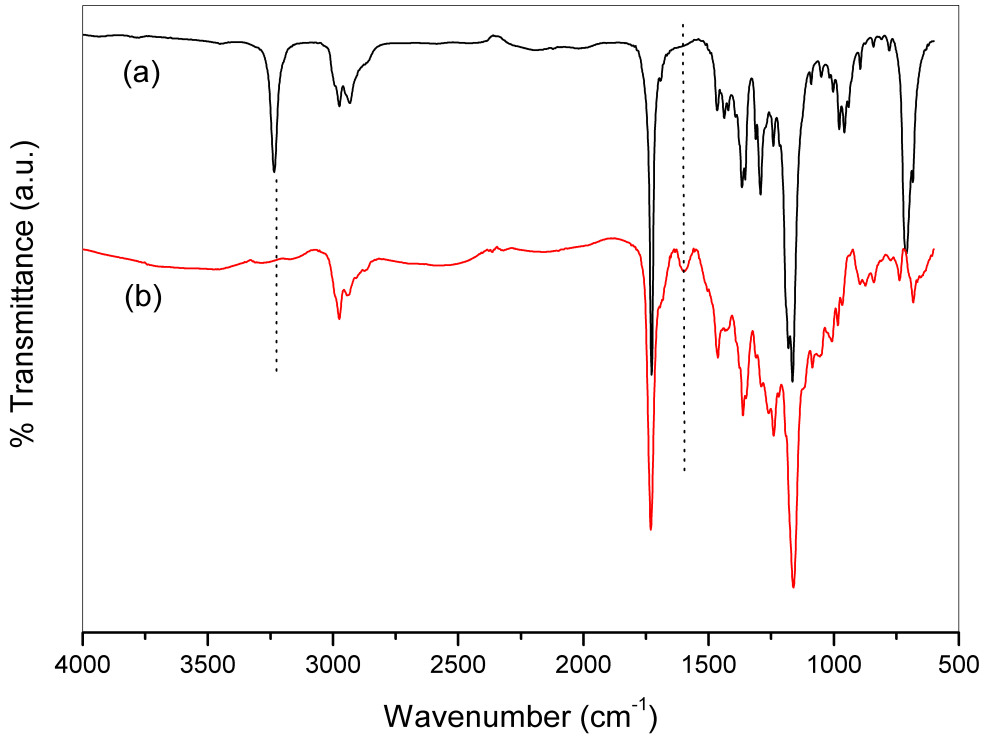

Figure 4.7. ATR spectrum of monomer (1), (a) and its polymer, poly(1), (b).

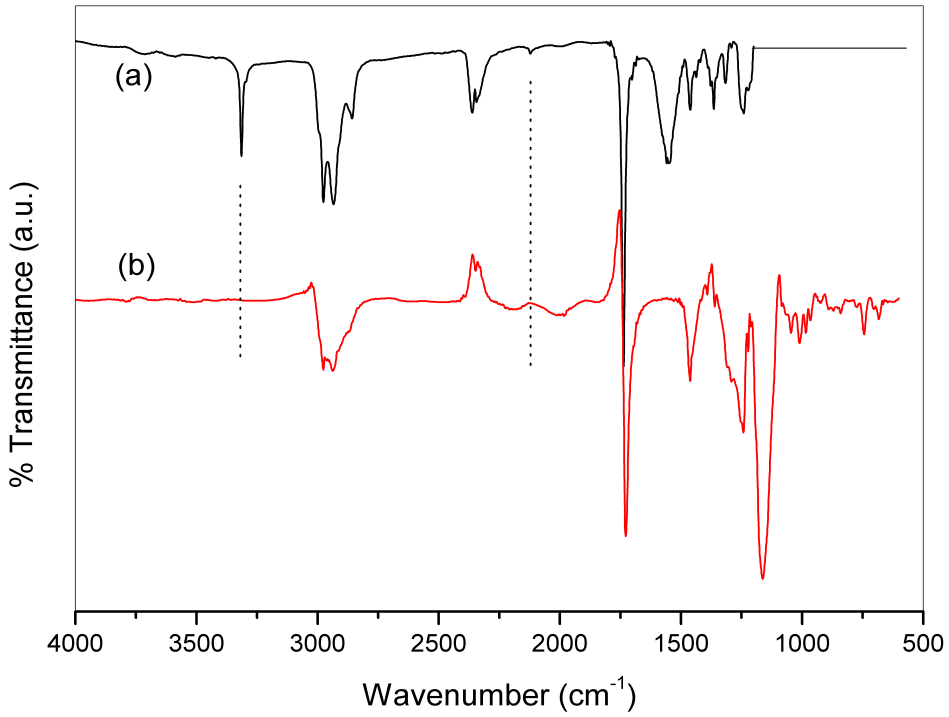

Figure 4.8. FT-IR spectrum of monomer (2),(a) and ATR spectrum of its polymer, Poly(2), (b).

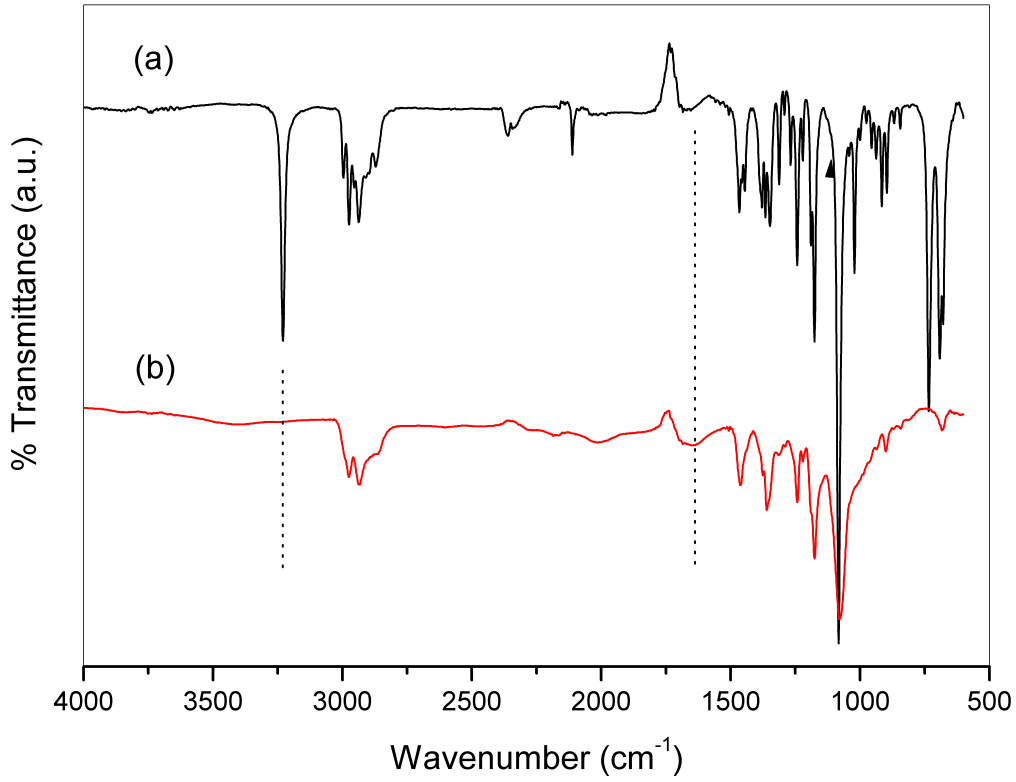

Figure 4.9. ATR spectrum of monomer (3), (a) and its polymer, poly(3), (b).

4.2.2. Properties of the Polymers

The morphology of the polymers was investigated by X-ray diffraction analysis. Figure 4.10 shows X-ray powder patterns of the polymers. Among them, poly(1) run 13 gave a sharp peak providing highest crystallinity when compared with other runs. Poly1 run 12 and poly2 showed a broad peak indicating typical amorphous material and maybe some crystalline part. Differently, poly3 displayed 2 weak shoulder indicating existence of somewhat crystalline part in the polymer chain.

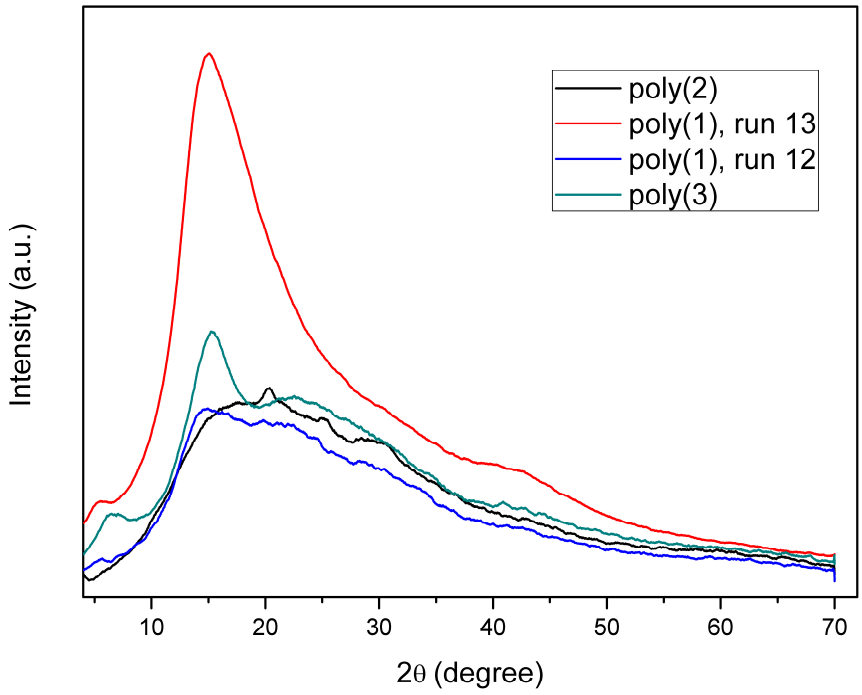

Figure 4.10. X-ray Powder patterns of poly(1) run 12, poly(1) run 13, poly(2) and poly(3).

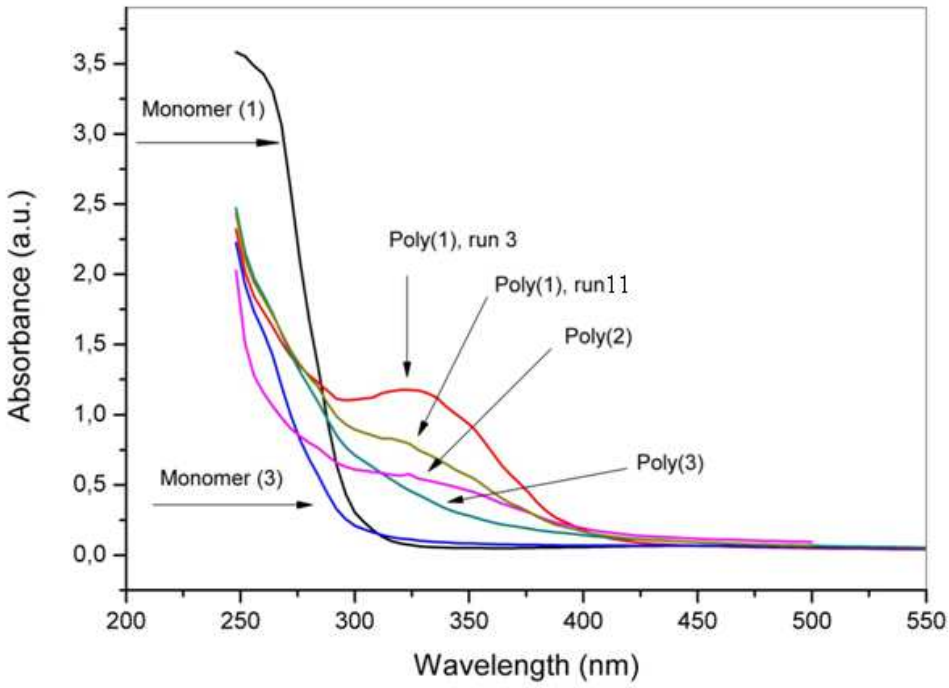

Figure 4.11. UV-Vis spectra of monomer(1), monomer(3) and poly(1), poly(2) and poly(3) run18 in dilute $CHCl_3$ solution.

Figure 4.11 illustrates the Ultraviolet/Visible (UV/Vis) spectra of poly(1)-poly(3) and their monomers obtained in $CHCl_3$. None of the monomers show any absorption wavelength longer than 300 nm. However, the polymers display broad absorptions near visible spectral region, with absorption maxima about 325 nm extending to 400 nm. This is specific absorption of conjugated backbone in the polymer chain. Whereas poly(1) and poly(2) show an absorption max. at 324 nm, poly(3) shows very low absorptivity. This can be due to the configuration changes due to cis-trans isomerization in double bonds reducing the effective conjugation lengths along the polyacetylene chain. This effect is seen some poly(1) runs. For example, poly(1), run11 has molecular weight 336900 and poly(1) run 3 has 383700. Although two polymer nearly have same molecular weight, one of them show a high absorption whereas the other show very low absorption due to conformation of polymer backbone and pendant groups.

Thermal characteristics of polymers were investigated by thermal gravimetric analysis (TGA) and the resultant thermograms are presented in Figure 4.12.

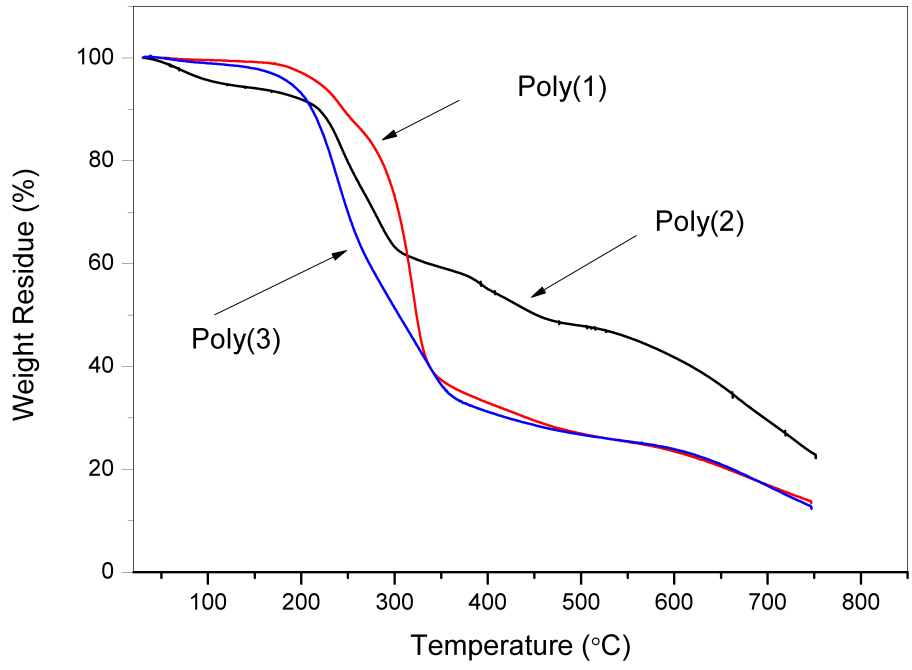

Figure 4.12. TGA curves of poly(1)-poly(3) measured at heating rate of 10.0°C/min in nitrogen at 20.0 ml/min.

The onset of decomposition at which 5% weight loss was observed for poly(1) and poly(3) occurred at around 188-219ºC. Above 220°C remarkable weight losses deriving from the thermal decompositions of the TEMPO moiety and the main chain. And all the polymer backbone is almost completely decomposed when the temperature reaches to 750 °C. Interestingly, poly(2) loses 5% of its weight around 115ºC and 50% weight loss is seen at 452°C whereas poly(1) and poly(3) show 50% weight loss at 323ºC. According to these results, increase in the monomer molecular weight seems to add greater thermal stability to the polymer. These analyses show that these polymers have good thermal stability to be used as an electrode material.

The DSC thermograms of polymers are presented in Appendix B. Poly(1), run 2 show a glass transition temperature of (Tg) near 72°C and T_m (melting temperature) at 96°C whereas the polymer with same structure but polymerized under different conditions, poly(1) run 3 displays no T_g. These differences may be arising from the differences in polymer backbone structure (different ratios of cis-cisoid, trans-cisoid and trans-transoid double bond arrangements in the polymer backbone). And Poly(2) and poly(3) show no Tg value at that temperature range.

4.2.3. ESR and Magnetic Characterizations

ESR spectrum of monomer(1) in $CHCl_3$ shows a characteristic nitroxide triplet at around g=2.0065 with a nitrogen hyperfine value (A_N) of 15.429 G. The spectrum is given in Fig. 4.13.

Figure 4.14 shows the electron spin resonance (ESR) spectra of poly**(1)**, poly**(2)** and poly**(3)** in the solid state. All the ESR spectra of the polymers exhibit singlet signals based on the TEMPO radical with *g*-factor of 2.00878, 2.00935, 2.01235 respectively, which of are nearly closer to 2.00935 for a typical nitroxyl radical of the TEMPO crystal. Poly(3) exhibits slightly larger *g*-factor than TEMPO itself. The interaction of radical group with polymer backbone can probably cause this small increase in the *g*-factor of poly(3) [86].

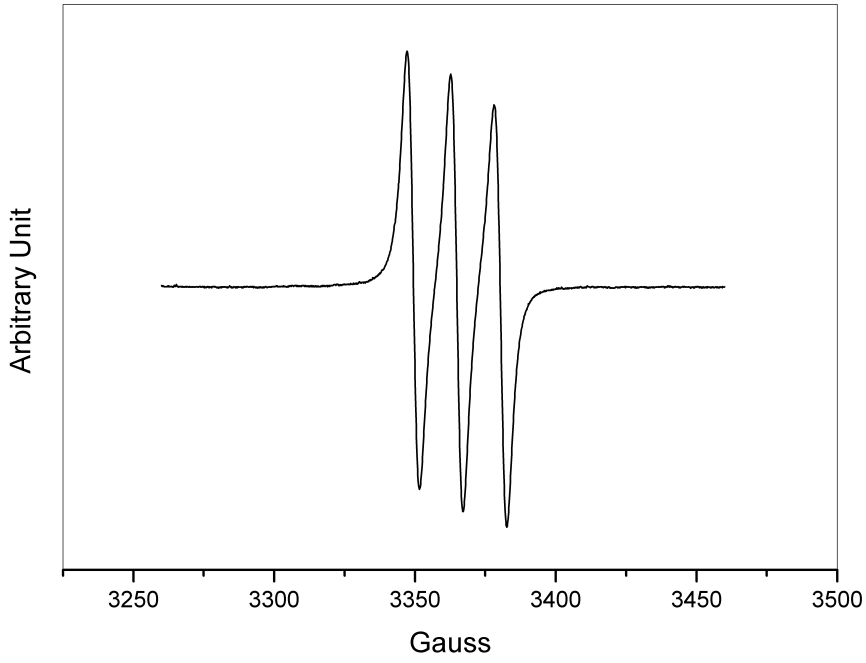

Figure 4.13. ESR spectrum of monomer (1) in $CHCl_3$.

The polymers poly**(1)**, poly**(2)** and poly**(3)** exhibit spin concentrations in the range of 2.164×10^{21}, 1.282×10^{21}, 2.165×10^{21} spins/g (obtained from ESR spin count experiments), respectively, indicating that quantitative amount of free radicals per monomer unit was successfully obtained during polymerization, except for poly(2). Table 4.2 summarizes the ESR data of polymers and Fig. 4.14 shows the sharp singlet signals of polymers.

Table 4.2. ESR data of polymers.

Polymer	**Number of Spins per Monomer Unit**	**Spin Concentration**	**ESR *g*-factor**
Poly(1)	0.9	2.164×10^{21}	2.00878
Poly(2)	0.45	1.282×10^{21}	2.00935
Poly(3)	0.96	2.165×10^{21}	2.01235

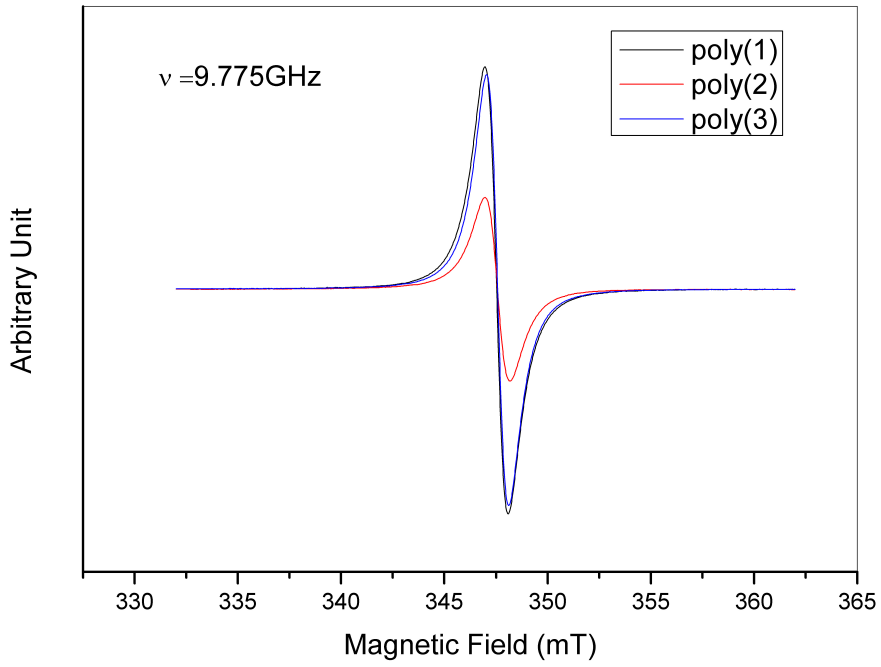

Figure 4.14. ESR spectrum of poly(1)-poly(3) measured in the powder state.

In addition to this method, spin concentration and magnetic property of poly(1) was determined from the slope of the Curie plots whose magnetic data were corrected for the diamagnetic contribution of the sample holder.

The magnetic susceptibility of poly(1) was obtained in the temperature range of 15–300 K. The temperature dependence of the molar magnetic susceptibility (χ_g) and $\chi_g T$ are shown in Fig. 4.15. The temperature variable dependence of χ_m was fitted by the relation of $\alpha+C/(T-\theta)$ where C is the Curie constant, θ is the Weiss constant and α is temperature independent susceptibility [100]. From this fitting process, C=0.00132 ± 0.0000008(emuK/g.Oe), α=0.00002 ± 0.000000007 and θ= −2.294±0.008 were determined. In here, there is temperature independent paramagnetism (α). This can be originated from that when the ground state couples with excited states or when there are itinerant (conducting) electrons and due to the orbital moments of electrons. In this temperature range, from these values it is resulted that there can be a small antiferromagnetic interaction in the structure. The magnetic interaction in such a magnetic behavior can be between localized magnetic moments.

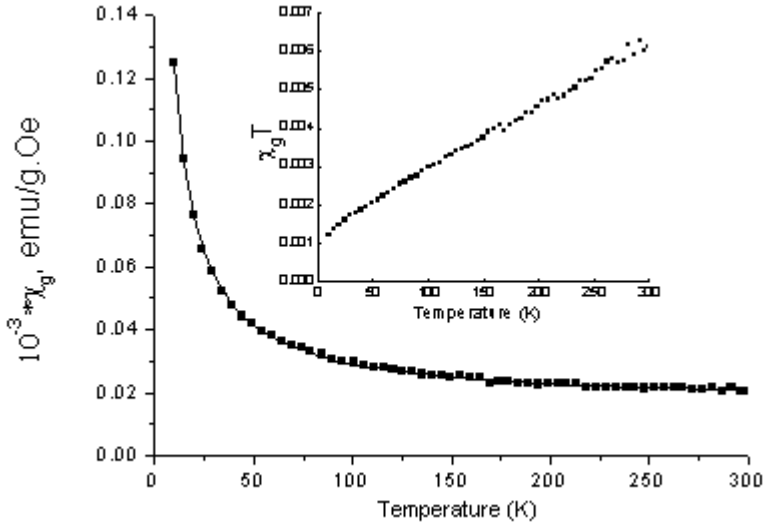

Figure 4.15. The temperature(K) dependence of the molar magnetic susceptibility χ_g for poly(1).

Solid line in Figure 4.15 represents a fit by the Curie–Weiss law. Inset shows the temperature dependence of $\chi_g T$ and fitting line.

$$C = \frac{N\mu_{eff}^2}{3k_B} \qquad \text{(Equation 1)}$$

where $\mu_{eff} = g\sqrt{S(S+1)}\mu_B$, g = 2, S = 1/2, μ_B = 0.9274x10^{-20} erg/G, k_B = 1.38x10^{-16} erg/K.

Using the C value found with simulation and substituting it in Equation 1, spin concentration of poly(1) was found as N_1 = 2.123x10^{21}/g. And this radical concentration values almost agreed with tested ESR data of poly(1).

4.2.4. Morphology of Polymer-Carbon Composites

To investigate the morphology of polymer-carbon composites scanning electron microscopy (SEM) was used and SEM pictures of poly(1) and poly(1)-graphite-PVDF(2:7:1) composite are shown in Figure 4.16.

SEM image shows that the morphology of poly(1) exhibits a lot of pores, like honeycomb sturcture. Differently, the morphology of composite has a flat, sharp irregular particles of graphite as seen in Figure 4.16 (b). The polymer and PVDF seem to coat the surface of graphite particles uniformly. Figure 4.16 (c) shows some fiber like

material on the surface of the material. This can be due to the dispersed PVDF binder mixed with polyacetylene. The graphite particle size appears to be quite large (> 5µm).

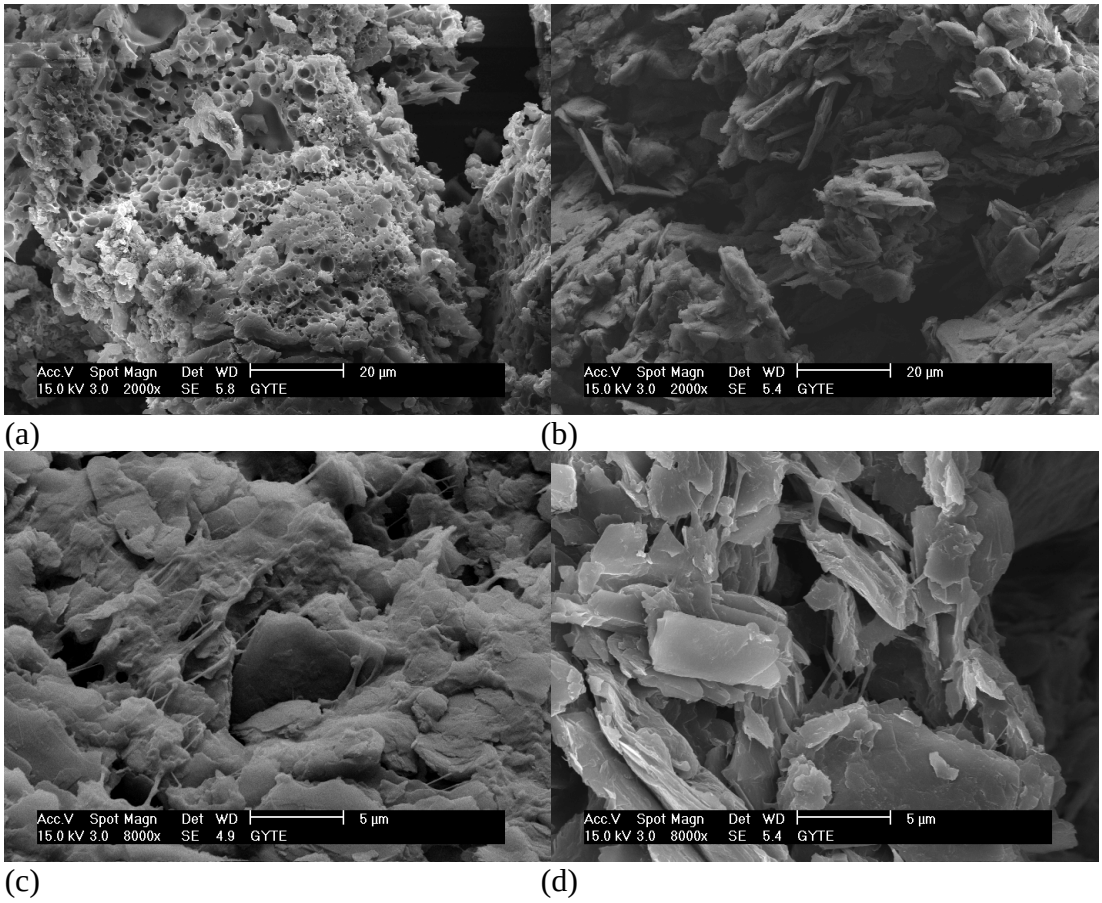

Figure 4.16. SEM images of :(a) poly(1), (b), (c), (d) polymer-graphite-PVDF composite.

4.2.5. Electrochemical Characterization of Polymers

Poly(1) and the graphite-poly(1) composite were characterized by cyclic voltammetry (CV) (Figures 4.17 and 4.18, respectively. Poly(1) and graphite-poly(1) composite samples were attached to a platinum micro electrode using a conducting gel, and a platinum wire counter electrode and Ag/AgCl reference electrode were used.

The first thing to be realized is that there is fully reversible oxidation and reduction based on TEMPO radical. So, these materials can display a great potential to be used as electrode active materials. Poly(1) exhibited an oxidation peak at 1.002 V vs Ag/Ag^+ and a reduction peak at 0.946V, while carbon composite of poly(1) shows corresponding oxidation peaks at 1.017 V vs Ag/Ag^+ and a reduction peak at 0.923 V.

Poly(2) dissolved in the electrolyte solution showed different oxidation peaks at 0.661 and corresponding reduction peaks at 0,645. The distances between the oxidation and reduction peaks of poly(1), carbon composite of poly(1), and poly(2) are 0.056, 0,094, 0.016, respectively. When these values are compared with first generation cathode active material, PTMA with a value of 0.146 V [1,81,82], they are very small. This means that the electrode reaction rates of the polymers are much higher. This may lead to production of rechargeable batteries which can be charged and discharged at a faster rate.

The reason for the oxidation and reduction potentials of poly(1) and its carbon composite are higher than standard value of TEMPO radical (around 0.6 V vs Ag/Ag^{+}) is that CV analyses were run in solid phase for poly(1) and its composite whereas the CV analysis for TEMPO was performed in the solution phase.

The increase in the gap between oxidation and reduction peak potentials of composite compared to pure poly(1) is probably caused by the use of a thicker composite pellet sample during measurement and by presence of more diverse and different microenvironments around the nitroxide moiety in the bulk of the composite compared to pure poly(1). The electron transfer reaction will be difficult on thicker electrodes although good reversibility is maintained.

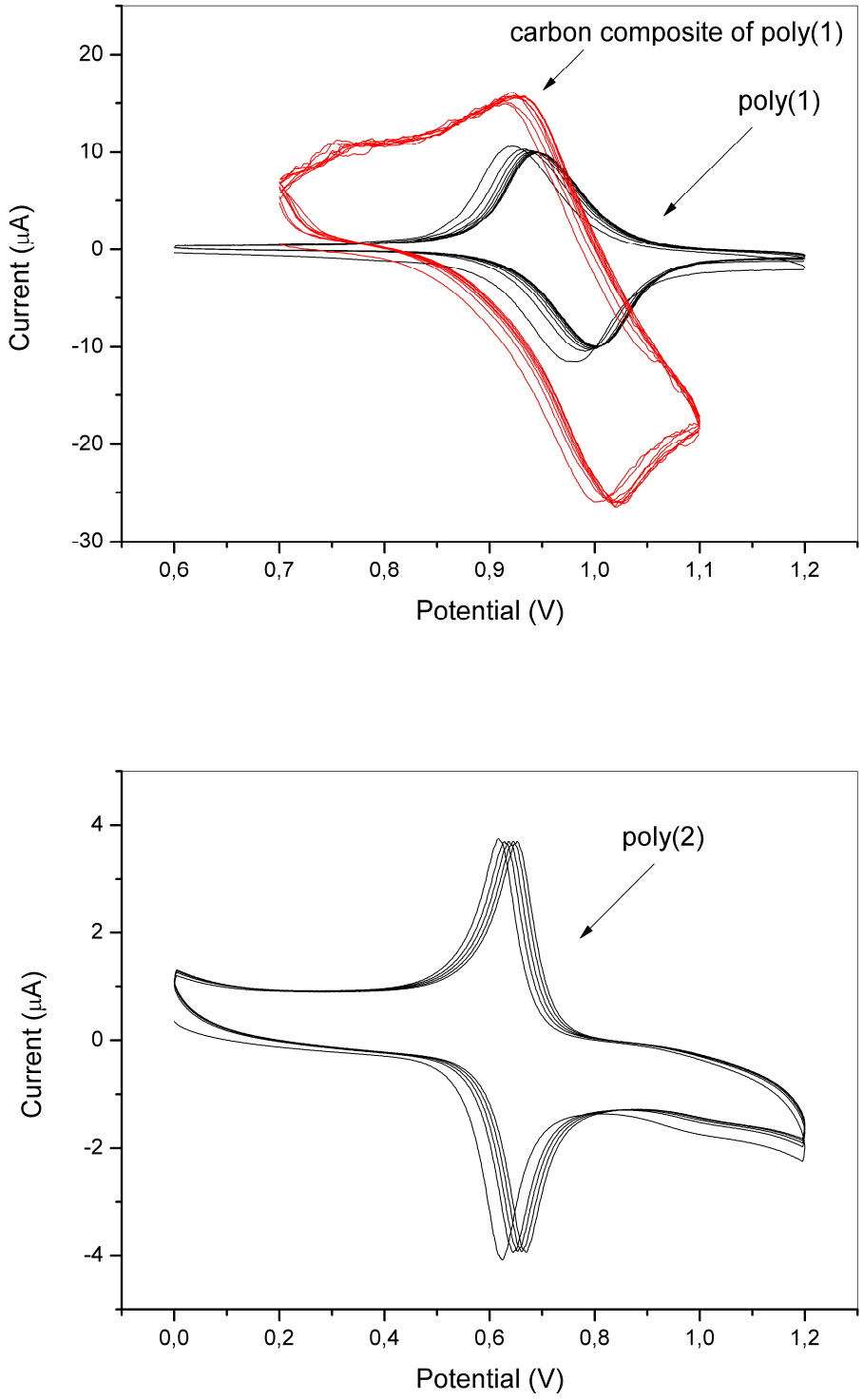

Figure 4.17. Cyclic voltagrams of poly(1), composite of poly(1), and poly(2) measured at a scan rate of 0.05 V/s vs Ag/Ag^{+} in TBAP solution.

4.2.6. Charge/Discharge Properties of the Cells

It is expected from a battery containing this radical as a pendant group display constant voltage plateau at the range of 3.5-3.7 V. Because TEMPO radical has a redox potential of 3.6 V vs Li anode. TEMPO moiety in the polymer is oxidized to oxoammonium salt during the charging process at the cathode which has to be neutralized by a counter-ion from the electrolyte (PF_6^- in our case)and goes back to its radical form during the discharging process by reverse reaction as it is seen Scheme 3.5.

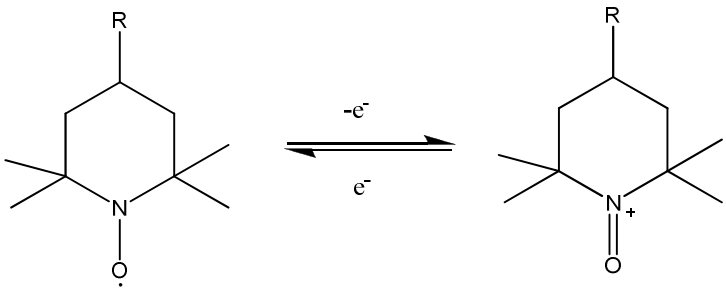

Scheme 3.5. Charge/discharge processes.

Figure 4.18 displays the charge/discharge curves of the coin cell fabricated using poly(2) as cathode and Li metal as cathode. It had an initial open circuit voltage (OCV) 2.66 V before testing started. The cell capacity was measured with constant current charge and discharge rate of 0.1 mA at a voltage range of 2.0 to 4.2, respectively, versus Li/Li^+. The electrode area and weight were 2.83 cm^2 and 2.6 mg active material (polymer).

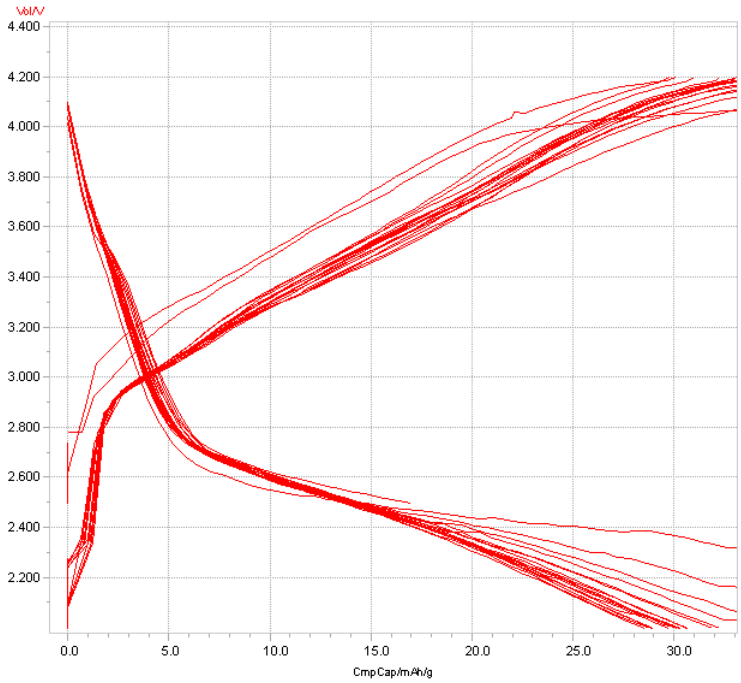

Figure 4.18. Charge-discharge curve of poly(2) at a current charge/discharge rate of 0.1 mA with a cell voltage of 2.0 to 4.2V.

During charging process the voltage sharply increased from 2.2 to 3 V at a range of 0-4 mAh/g cell capacity, followed by a sloping curve until reaching cutoff voltage 4.2 V. The cycle was completed in 52 minute. The cell capacity reached to 33.3 mAh/g. During the discharge process, the voltage reduced sharply from 4.2 to 2.8 V within 0-5 mAh/g cell capacity, then fall to 2V with a sloping curve, again. Sloping behavior is probably due to non-stochiometric ion insertion into the electrodes [101-103]. It may not exhibit uniform counter-ion or electron distribution.

The initial discharge process displayed a cell capacity of 29 mAh/g in 45 minute. The measurement showed that cell displayed a good durability after at least 10 cycles with efficiency of 87% (Charge/Discharge). The theoretical capacity of the cell is 139.4 Ah/kg as calculated from Equation 2 below.

$$\text{Capacity (mAh/g)} = \frac{96500}{3600(MonomerMwt/1000)} \quad \text{(Equation 2)}$$

The observed discharge capacity was much lower than theoretical one. The reason are really not known, but it may be due to the low spin concentration which has a value of 1.282×10^{21} spins/g, amounting to 0.45 spin/repeating unit instead of 1.0 spins per repeating unit (see the Table 4.2). Aggregation in the polymer may also be effective in this observed low discharged capacity due to the presence of sites which are not accessible to the counter ion and therefore not oxidized during charging process.

The capacity of the battery can vary depending on the current charge/discharge rate. Figure 4.19 shows this relationship. The cell was tested with constant current drain 0.05 mA at a voltage range of 2.0 to 4.2. The battery reached 4.0 V in 180 minutes and displayed charge capacity 54 mAh/g and it was discharged back to 2.0 V in 132 minutes with a discharge capacity of 45 mAh/g. The efficiency is 83.5% (Charge/Discharge).

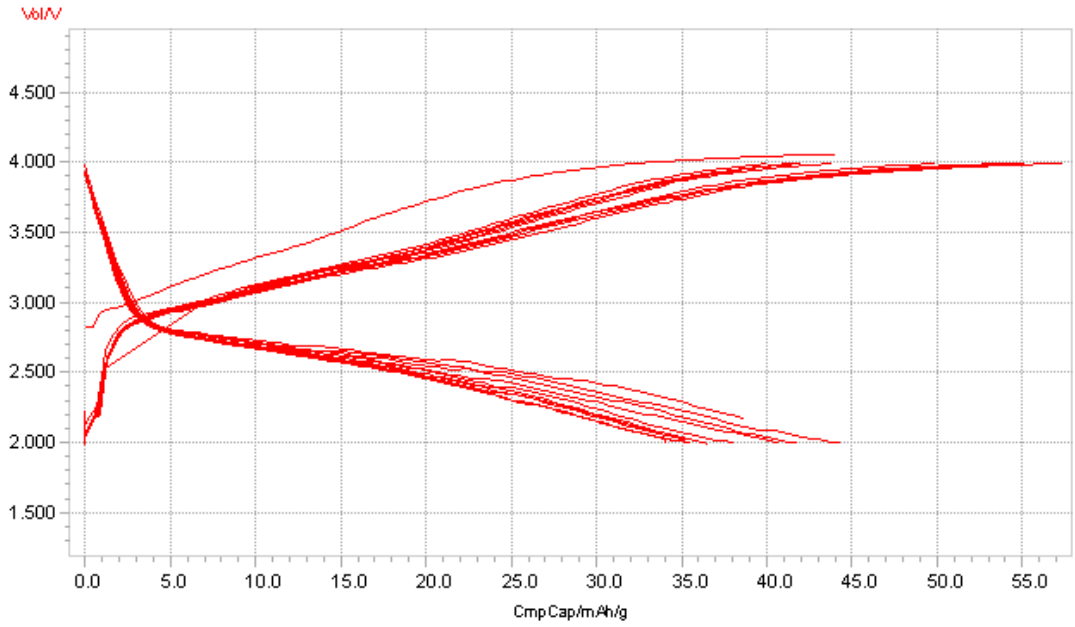

Figure 4.19. Charge-discharge curve of poly(2) at a current charge/discharge rate of 0.05mA with a cell voltage of 2.0 to 4.2V.

This results show that charge and discharge capacities gradually decreased with increasing current, which can be attributable to the polarization of TEMPO. The expected cell voltages could not be attained in the coin cells probably due to the fast ohmic voltage drop which may be related to cell construction.

Other coin cells constructed with polymer composites as cathodes and graphite as anodes were unsuccessful as they had extremely low specific capacities.

Since the poly(1) and poly(3) were soluble in electrolyte solution ethylene carbonate / diethylcarbonate (30:70 vol%), unfortunately they were not applied as electrode material in the battery construction.

CHAPTER 5

CONCLUSION

In this work, we successfully synthesized three new TEMPO containing functional polyacetylenes and studied their properties. The reactions proceeded smoothly, and all the desired monomers were obtained at moderate yields (63-79%). The formed polymers were thermally stable up to 180°C and some of them soluble in common solvents like THF, $CHCl_3$, CH_2Cl_2. The polymers were obtained with number-average molecular weights upto387300 and with up to 64% yield. The effects of polymerization conditions, such as concentration, monomer/catalyst ratio, catalyst/cocatalyst ratio, cocatalyst type, solvent, an temperature on the polymer properties have been investigated. The conditions such as temperature, monomer concentration and cocatalyst type have been found to show no significant effect on polymer molecular weights. Polymers with reasonable yields which are THF and EC/DEC insoluble were obtained when 0.2 M solution of the monomer in THF polymerized with 0.002M $[Rh(nbd)Cl]_2$ /LDA catalyst/cocatalyst system in a molar ratio of 1/100 at 35°C.

The ESR spectrum of polymers of monomer(1) and monomer(3) exhibited a singlet and quantitative amounts of free radicals based on the TEMPO moiety with ca. 1 spin per repeating unit. But the polymer of monomer(2) displayed 0.45 spin/repeating unit. Since the poly(1) and(3) were soluble in electrolyte solution they were not used to construct electrodes. Only more electrolyte insoluble poly(2) was tested as a cathode active polymer in a battery.

The coin cell constructed had a 2.66 V OCV and discharged with 0.1 mA during 45 minute up to 4 V. It displays 29 mAh/g, corresponding to 20.8% of the theoretical

capacity value (139.4 Ah/kg). The measurement showed that cell displayed a good durability after at least 10 cycles with efficiency of 87% (Charge/Discharge). Anticipated results from the coin cells have not been realized to the full extent probably due to lower than expected spin concentration on the polymer and due to poor counter-ion insertion into the polymer composite used as the cathode. Cell construction and related ohmic reduction of cell potential may also have an important effect. If these problems are removed successfully, organic radical batteries with high capacity can find a wide range of potential applications in future. This needs trial of new polymeric structures, electrode material compositions and different cell constructions.

APPENDIX A

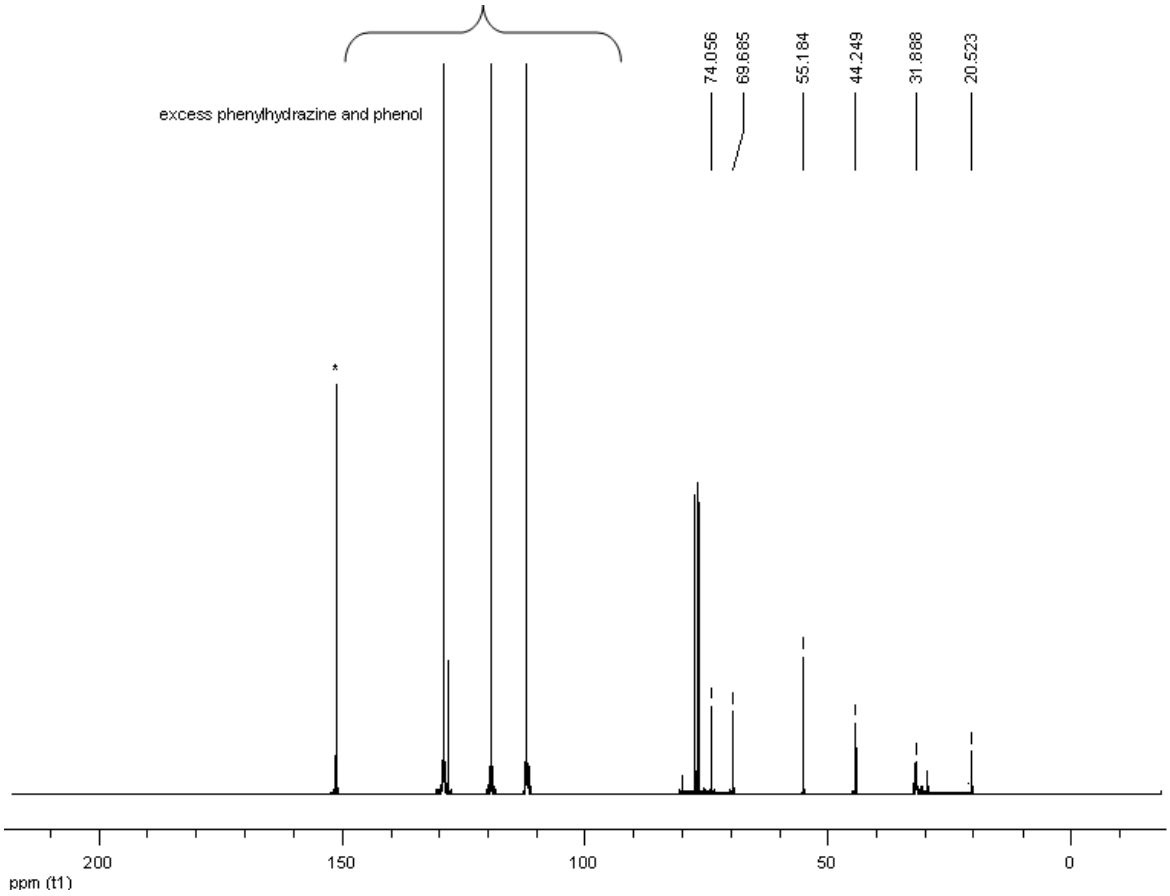

^{13}C NMR spectrum of monomer(3).

APPENDIX B

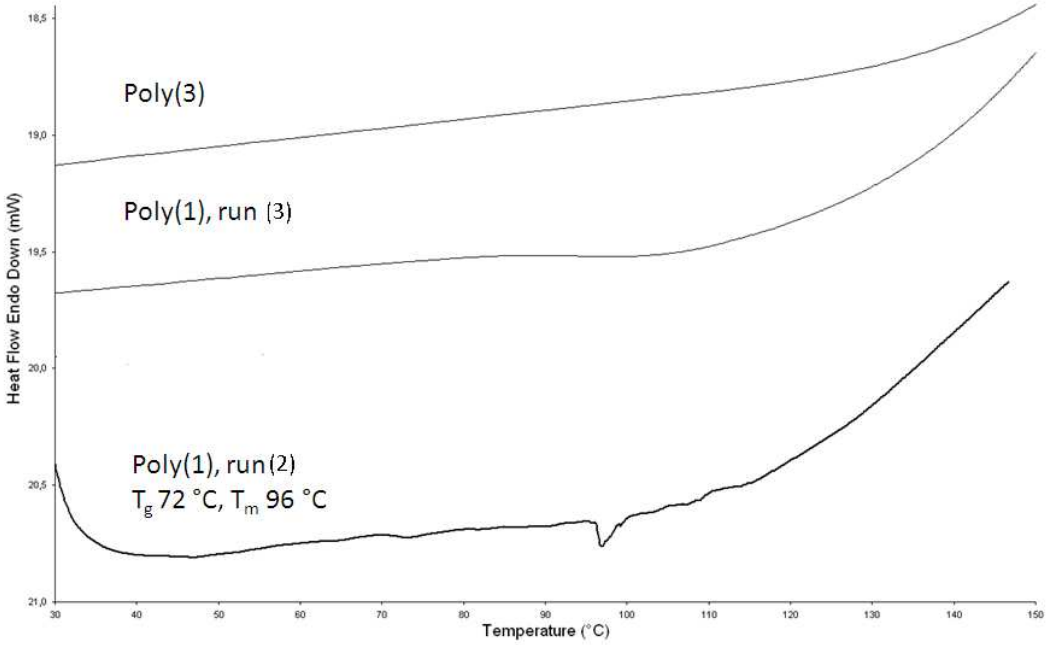

DSC curves of poly(1),run 2, run (3) and poly(3).

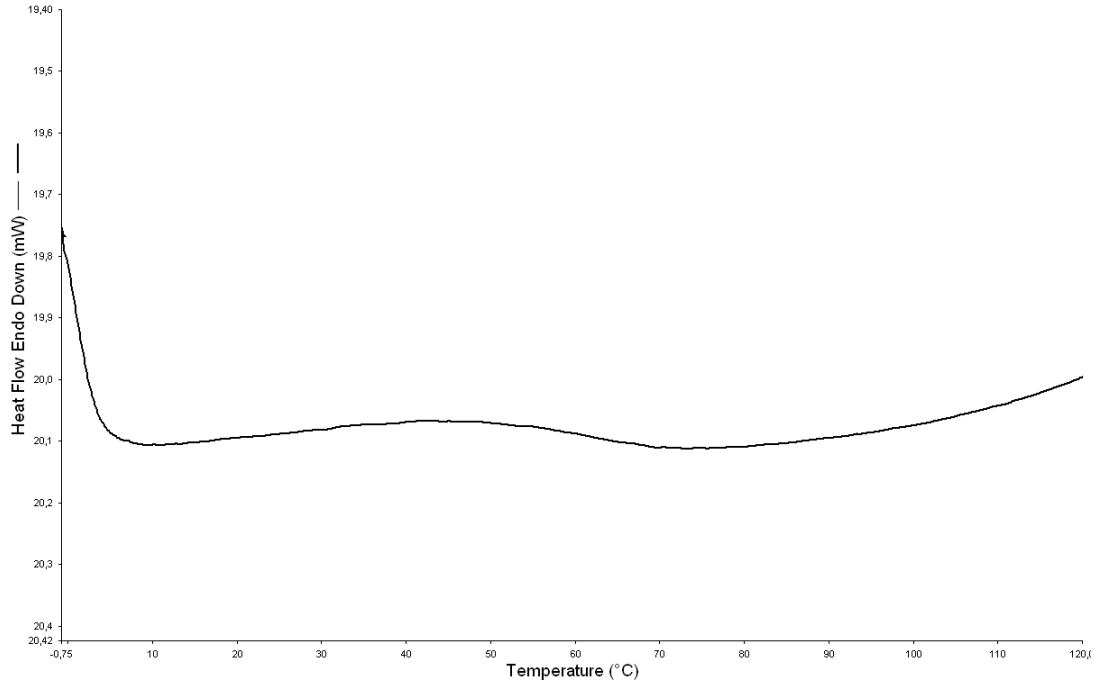

DSC curve of poly(2).

REFERENCES

[1] Nakahara, K.; Iwasa, S.; Satoh, M.; Morioka, Y.; Iriyama, J.; Suguro, M.; and Hasegawa, E., Chem. Phys. Lett., 359 (2002) 351.

[2] Suga,T.; Konishi, H.; Nishide, H., Chem. Commun., (2007) 1730.

[3] Suga, T.; Yoshimura, K.; Nishide, H., Macromol. Symp., 245-246 (2006) 416.

[4] Suga,T.; Pu, Y. J.; Oyaizu, K.; Nishide, H., Bull. Chem. Soc. Jpn., 77 (2004) 2203.

[5] Nishide, H.; Suga, T.; The Electrochemical Society Interface, 14 (2005) 32.

[6] Shirakawa, H.; Louis, E. J.; MacDiarmid, A. G.; Chiang, C. K.; and Heeger, E. J., J. Chem. Soc. Chem. Commun., (1977) 578.

[7] McInnes, D.; Druy, M. A.; Nigrey, P. J.; Nairns, D. P.; MacDiarmid, A. G., and Heeger, A. J., J. Chem. Soc. Chem. Commun., (1981) 317.

[8] Tang, C. W. and Van Slyke, S. A., Appl. Phv.t. Lett., (1987) 51913.

[9] Burroughes, J. H.; Bradley, D. D. C;, Brown, A. R.; Marks, R. N;, Mackay, K.; Friend, R. H.; Burns, P. L.; Holmes, A. B., Nature 347 (1990) 539 – 541.

[10] Sariciftci, N.S.; Smilowitz, L.; Heeger, A.J.; and Wudl, F., Science 258(5087) (1992) 1474-1476

[11] Braun, D.; Heeger, A. J., Appl. Phys. Lett., 58 (1991) 1982.

[12] Mortimer, R .J., Chem. Soc. Rev., 26 (1997) 147.

[13] Somani, P. R.; Radhakrishnan, S., Mater. Chem. and Phys., 77 (2002) 117.

[14] Orellana, M.; Arriola, P.; Rio, R. D.; Schrebler, R.; Cordova, R.; Scholz, F. Kahlert, H., J. Phys. Chem. B, 109 (2005) 15483.

[15] Application Note 3958, Battery Fuel Gauges: Accurately Measuring Charge Level, Dec 22, 2006.

[16] Bittner, H. F.; Badcock, C. C., J. Electrochem. Soc., 130 (1983) 193C.

[17] Furukawa, N., J. Power Sources, 51 (1994) 45.

[18] Santos, J.S.A., Sequeira, C. A. C., in Chemistry and Energy I (Ed: C. A. C. Sequeira), Elsevier, Amsterdam (1991) 13.

[19] Kennet, P. D.; Bullock, K. R.; Fiorino, M. E., Interface 4 (1995) 3.

[20] Volodarsky, L. B.; and Reznikov, V. A., Synthetic Chemistry of Stable Nitroxides, CRC Press, Boca Raton, FL (1993).

[21] Iwamoto, T.; Masuda, H.; Ishida, S.; Kabuto, C.; Kira, M. J. Am. Chem. Soc., 125 (2003) 9300-9301.

[22] Petr, A.; Dunsch, L.; Koradecki, D.; Kutner, W. J. Electroanal. Chem., 300 (1991) 129-146

[23] Anderson, C. D.; Shea, K. J.; Rychnovsky, S. D., Org. Lett., 7 (2005) 4879-4882.

[24] Ferreira, P.; Phillips, E.; Rippon, D.; Tsang, S. C.; Hayes, W. J. Org. Chem., 69 (2004) 6851-6859.

[25] Tanyeli, C.; Gümüş, A. Tetrahedron Lett. 44 (2003) 1639-1642.

[26] MacCorquodale, F.; Crayston, J. A.; Walton, J. C.; Worsfold, D. J. Tetrahedron Lett. 31 (1990) 771-774.

[27] Nishide, H., Adv. Mater., 7 (1995) 937-941.

[28] Rajca, A., Chem. Rev., 94 (1994) 871-893.

[29] Iwamura, H.; Koga, N. Acc. Chem. Res., 26 (1993) 346-351.

[30] Fujii, A.; Ishida, T.; Koga, N.; Iwamura, H. Macromolecules, 24 (1991), 1077-1082.

[31] Semmelhack, M. F.; Schmid, C. R. J. Am. Chem. Soc., 105 (1983) 4492.

[32] Miyazawa, T.; Endo, T.; Shiihashi, S.; Okawara, M.; J. Org. Chem., 50 (1985) 1332.

[33] Osa, T.; Akiba, U.; Segawa, I.; Bobbitt, J. M. Chem. Lett., (1988) 1423.

[34] Merz, A.; Reitmeier, S. J. Chem. Soc. Chem. Commun., (1990) 1054.

[35] Merz, A.; Bachmann, H. J. Am. Chem. Soc., 117 (1995) 901.

[36] MacCorquodale, F.; Crayton, J. A.; Walton, J. C.; Worsfold, D. J. Tetrahedron Lett., 31 (1990) 771.

[37] Kaufman, F. B.; Schroeder, A. H.; Engler, E. M.; Kramer, S. R.; Chambers, J. Q. J. Am. Chem. Soc., 102 (1990) 483.

[38] Shirota, Y.; Kakuta, T.; Mikawa, H. Makromol. Chem. Rapid Commun., 5 (1984) 337.

[39] Iwakura, C.; Kawai, T.; Nojima, M.; Yoneyama, H. J. Electrochem. Soc., 134 (1987) 791.

[40] Bittner, H. F.; Badcock, C. C., J. Electrochem. Soc., 130 (1983) 193C.

[41] Shirota, Y.; Noma, N.; Kanega, H. Mikawa, H. J. Chem. Soc., Chem. Commun. (1984) 470.

[42] Kakuta, T.; Shirota, Y.; Mikawa, H. J. Chem. Soc., Chem. Commun. (1985) 553.

[43] Kaufman, F. B.; Schroeder, A. H.; Engler, A. H.; Kramer, E. M.; Chambers, S. R. J. Am. Chem. Soc., 102 (1990) 483

[44] Compton, R. G.; Day, M. J.; Ledwith, A.; Abu-Abdoun, I. I. J. Chem. Soc., Chem. Commun. (1986) 328.

[45] Compton, R. G.; Laing, M. E.; Ledwith, A.; Abu-Abdoun, I. I. J. Applied Electrochem., 18 (1988) 431.

[46] Hunter, T. B.; Tyler, P. S.; Smyrl, W. H.; White, H. S. J. Electrochem. Soc., 134 (1987) 2198.

[47] Visco, S.J.; Mailhe, C. C.; De Jonghe, L. C.; and Armand, M. B.; J. Electrochem. Soc., 136 (1989) 661.

[48] Visco, S. J.; Lui, M. and De Jonghe, L. C., J. Electrochem. Soc., 137 (1990) 1191-1192.

[49] Visco, S. J.; DeJonghe, L. C.; Ue, M. Denki Kagaku 62 (1994) 300.

[50] Doeff, M. M.; Lerner, M. M.; Visco, S. J.; and De Jonghe, L. C., J. Electrochem. Soc., 139 (1992) 2077.

[51] Doeff, M. M.; Visco, S. J.; and De Jonghe, L. C., J. Electrochem. Soc., 139 (1992) 1808.

[52] Tatsuma, T.; Sotomura, T.; Sato, T.; Buttry, D. A.; Oyama, N., J. Electrochem. Soc., 142 (1995) L182.

[53] Naoi, K; Kawase, K.; Mori, M.; and Komiyama, M. J. Electrochem. Soc., 144, (1997) L173.

[54] Pope, J.M.; Oyama, N., J. Electrochem. Soc., 145(1998) 1893.

[55] Pope, J.M.; Sato, T.; Shoji, E.; Oyama, N.; White, K.C.; and Buttry, D.A., J. Electrochem. Soc., 149 (7) (2002) A939.

[56] Liu, M.; Visco, S. J.; De Jonghe, L. C., J. Electrochem. Soc., 136 (1989) 2570.

[57] Liu, M.; Visco, S. J.; De Jonghe, L. C., J. Electrochem. Soc., 137 (1990) 750.

[58] Liu, M.; Visco, S. J.; De Jonghe, L. C., J. Electrochem. Soc., 138 (1991) 1891.

[59] Shirakawa, H.; Louis, E. J.; MacDiarmid, A. G.; Chiang, C. K.; Heeger, A. J., J. Chem. Soc., Chem. Commun. (1977) 578.

[60] Nova´K, P.; Müller, K.; Santhanam, K. S. V.; Haas, O., Chemical Reviews, 97 (1997) 207-281

[61] Caja, J.; Kaner, R. B.; MacDiarmid, A. G., J. Electrochem. Soc., 131 (1984) 2744.

[62] Armand, M. B. In Solid State Batteries; Sequeira, C. A. C., Hooper, A., Eds.; Martinus Nijhoff Publ.: Dordrecht, 1985, 363.

[63] Moliton, A.; Hiorns, R. C., Polym Int., 53 (2004) 1397–1412.

[64] MacDiarmid, A. G.; Nigrey, P. J.; MacInnes, D. F., Jr.; Nairns, D. P.; Heeger, A. J., Org. Coat. Plast. Chem., 44 (1981) 372.

[65] MacInnes, D. Jr., J. Chem. Soc., Chem. Commun. 317, 45, Chiang, C.K. 1981.

[66] Nagatomo, T, Polym.Commun., 22 (1983) 1454.

[67] Farrington, G.C.; and R. Huq., Jpn J Appl Phys, 22 (1985) L275.

[68] Nagatomo, T.; Ichikawa, C.; and Omoto, O., J Power Sources (1987) 14:3.

[69] Efimov, O.N., J. Electrochem. Soc., (1996)134 (2):305.

[70] MacInnes Jr., D.; Druy, M. A.; Nigrey, P. J.; Nairns, D. P.; MacDiarmid, A. G.; and Heeger, A. J., J. Chem. Soc., Chem. Commun., 1981, 317–319.

[71] Shinozaki, K.; Tomizuka, Y.; and Nojiri, A., J. Electrochem. Soc., 128 (1984) 1651.

[72] Shinozaki, K.; Tomizuka, Y.; Nojiri, A., Japanese Journal of Applied Physics, 2:23 (1984) L892-L894.

[73] C.K. Chiang, Polym. Commun., 22 (1981) 1454.

[74] MacDiarmid, A. G.; Chiang, J.-C.; Halpern, M.; Huang, W. S.; Krawczyk, J. R.; Mammone, R. J.; Mu, S. L.; Somasiri, N. L. D.; Wu, W. Polym. Prep., Am. Chem. Soc., Div. Polym. Chem, 25 (1984) 248.

[75] Kaner, R.B.; A.G. MacDiarmid; and R.J. Mammone, ACS Symp Ser., 242 (1984) 575.

[76] Farrington, G. C.; Huq, R., J. Power Sources, 14 (1985) 3.

[77] Farrington, G.C. ; DeNuzzio, J. ; Frydrych, D. ; Scrosati, B., J. Electrochem. Soc., 131 (1984) 7.

[78] Volodarsky, L. B.; Reznikov, V.A., Synthetic Chemistry of Stable Nitroxides, CRC Press, Florida, 1993.

[79] Nakahara, K.; Iwasa, S.; Satoh, M.; Morioka, Y.; Iriyama, J.; Suguro, M.; and Hasegawa, E., Chemical Physics Letters, 359 (2002) 351-354.

[80] Nishide, H.; Suga, T., Electrochem. Soc. Interface, 14 (2005) 32– 36.

[81] Nishide, H. ; Iwasa, S.; Pu, Y. J.; Suga, T.; Nakahara, K.; Satoh, M., Electrochim. Acta, 50 (2004) 827 –831.

[82] Satoh, M.; Nakahara, K.; Iriyama, J.; Iwasa, S.; Suguro, M., Rev. Int. Criminol. Police Tech. IEICE Trans. Electron., E87-C (2004) 2076.

[83] Nishide, H.; Koshika, K.; and Oyaizu, K., Pure Appl. Chem., 11:81 (2009) 1961-1970.

[84] Suga, T.; Konishi, H.; and Nishide, H., Chem. Commun., (2007) 1730–1732.

[85] Katsumata, T.; Satoh, M.; Wada, J.; Shiotsuki, M.; Sanda, F.; Masuda, T. Macromol. Rapid Commun., 27 (2006) 1206–1211,

[86] Katsumata, T.; Satoh, M.; Wada, J.; Masuda, Macromolecules, 40 (2007) 3136-3144.

[87] Katsumata, T.; Qu, J.; Shiotsuki, M.; Satoh, M.; Wada, J.; Igarashi, J.; Mizoguchi, K.; and Masuda, T., Macromolecules, 41 (2008) 1175-1183.

[88] Qu, J.; Katsumata, T.; Satoh, M.; Wada, J.; Masuda, T., Polymer 50 (2009) 391–396.

[89] Qu, J.; Katsumata, T.; Satoh, M.; Wada, J.; Igarashi, J; Mizoguchi, K.; and Masuda, T., Chem. Eur. J., 13 (2007) 7965 – 7973.

[90] Qu, J.; Fujii, T.; Katsumata, T.; Suzuki, Y.; Shiotsuki, M.; Sanda, F.; Satoh, M.; Wada, J.; Masuda, T.; 23:45 (2007) 5431-5445.

[91] Qu J; Khan F. Z.; Satoh M.; Wada J.; Hayashi H.; Mizoguchi K., Polymer 49 (2008) 1490–6.

[92] Qu J.; Morita R.; Satoh M.; Wada J.; Terakura F.; Mizoguchi K., Chem. Eur. J. 14 (2008), 3250–9.

[93] Ott I.; Schmidt K.; Kircher B.; Schumacher P.; Wiglenda T.; Gust R., J. Med. Chem. 48 (2005) 622.

[94] Zhang, W.; Tabei, J.; Shiotsuki, M.; Masuda, T., Polymer Bulletin 57 (2006) 463–472.

[95] Opsteen, J. A.; Van Hest, J. C. M., Chem. Commun., (2005) 57–59.

[96] Bogdan, A.; McQuade, D. T.; Beilstein Journal of Organic Chemistry 5 (2009) No, 17.

[97] Gheorghe, A.; Cuevas-Yañez, E.; Horn, J.; Bannwarth, W.; Narsaiah, B.; Reiser, O., Syntlett 17 (2006) 2767-2770.

[98] Anderson, J. E.; Corrie, J. E. T., J. Chem. Soc., Perkin Trans. 2 (1992) 1027-1031.

[99] Lee, Terry D.; Keena, F. W., J. Org. Chem. 40 (1975) 21.

[100] Earney, J.J.; Finn, C.P.B.; and Najafabadi, B. M., J. Phys. C: Solid St. Phys. 4 (1971) 1013-1021.

[101] Shacklette, L.W.; Maxfield, M.; Gould, S.; Wolf, J.F.; Jow, T.R.; and Baughman, R.H., Synthetic Metals, 18 (1987) 611 618.

[102] Shacklette, L.W.; Toth, J.E.; Murthy, N.S.; and Baughman, R.H., J. Electrochem. Soc., 132 (1985) 1529.

[103] Baughman, R.H.; Murthy, N. S.; Miller, G. G.; Shacklette, L.W.; and Metzger, R.M., J. Physique C3~ 44 (1983) 53.